Thermal decomposition of AIBN, Part B: Simulation of SADT value based on DSC results and large scale tests according to conventional and new kinetic merging approach

Bertrand Roduit[a,*], Marco Hartmann[a], Patrick Folly[b], Alexandre Sarbach[b], Pierre Brodard[c], Richard Baltensperger[c]

[a] AKTS AG, TECHNOArk 1, 3960 Siders, Switzerland[1]
[b] Armasuisse, Science and Technology Centre, 3602 Thun, Switzerland
[c] University of Applied Sciences of Western Switzerland, Bd de Pérolles 80, 1705 Fribourg, Switzerland

A R T I C L E   I N F O

A B S T R A C T

The paper presents the results of the common project performed with the Federal Institute for Materials Research and Testing, Berlin, Germany (BAM) concerning the comparison of the experimental results with simulations based on the application of the kinetic-based method and heat balance of the system for the determination of the self accelerating decomposition temperature (SADT). The substantial potential of the kinetic-based method is illustrated by the results of the simulation of SADT of azobisisobutyronitrile (AIBN). The influence of sample mass and overall heat transfer coefficient on the SADT values were simulated and discussed. Simulated SADT values were verified experimentally with a series of large-scale experiments (UN test H.1 [1]) performed with packaging of 5, 20 and 50 kg of AIBN in an oven at constant temperatures. Additionally, the results of small-scale test H.4 for SADT determination based on the heat loss similarity as described in details in the UN Manual [1] were compared with the simulated data based on kinetic approach. The paper presents also the basic principles of a new kinetic analysis workflow in which the heat flow traces (e.g., DSC) are simultaneously considered with results of large-scale tests as e.g., H.1 or H.4. Application of the newly proposed kinetic workflow may increase accuracy of simulations of SADT based on results collected in the mg-scale and considerably decrease the amount of expensive and time consuming experiments in kg-scale tests.

1. Introduction

Some chemicals have the potential to cause fires or explosions, and, as hazardous materials, are handled with appropriate care to minimize accidents. This category of hazardous materials includes a group of chemical substances called "reactive or self-reactive chemicals" which may initiate exothermic decomposition by themselves without reacting with oxygen in air. The estimation of the hazard probability, especially for packaged materials during transport conditions, is commonly performed using thermal hazard indicators such as the self accelerating decomposition temperature (SADT). The determination of SADT is based on the monitoring of the temperature of the sample with the mass m, volume V, surface area S, density (or bulk density) ρ, and specific

heat capacity C_p, with a uniform initial temperature T_0 and packed into a vessel of arbitrary shape. At time t_0, the surrounding temperature of the investigated material is increased to T_e which initiates the heat transfer between the packaged material and its surroundings, characterized by a heat transfer coefficient h. The SADT, as defined by the United Nations SADT test H.1 [1], is the lowest ambient temperature at which the center of the material within the package heats to a temperature $6\,^\circ C$ higher than the environmental temperature T_e after seven days or less. This period is measured from the time when the temperature in the center of the packaging reaches $2\,^\circ C$ below the ambient temperature. The determination of SADT can be reliably performed applying UN test H.1 [1] with a series of large-scale experiments performed with the packaging in an oven at constant temperatures. Each test, performed at a new temperature, (according to the UN Recommendations, the step of the oven temperature variations amounts to $5\,^\circ C$) requires a new large-scale packaging. Despite its reliability, this procedure, based on a series of large-scale experiments, is rarely used, because it is rather expensive, time-consuming and, in

certain cases, quite dangerous due to thermal safety and toxicity reasons. Another limitation is related to the relatively common situation when only a small amount of the investigated material is available at the early stages of a project. Taking into account all the issues presented above, it seems fully understandable that there is an important need of other reliable, faster, safer and cheaper test methods requiring smaller amounts of reactive materials and applicable at the laboratory scale (mg or g). Due to the fact that significant amount of heat is evolved during the decomposition of self-reactive chemicals their thermal properties are frequently investigated in laboratory at mg- or g-scales under non-isothermal or isothermal conditions using differential scanning calorimetry (DSC) or, more sensitive, heat flow calorimetry (HFC). The elaboration of the heat flow data monitored by these both techniques allows determination of the kinetic parameters of the decomposition process which describe the rate of the heat generation in the conditions of the ideal heat exchange with the surroundings. Because these tests are performed at a small scale, a scale-up is necessary. In kg-scale, due to increasing sample mass, the conditions of the heat exchange with the environment significantly change what, in turn, may considerably increase the reaction rate and the spatial evolution of the sample temperature which depends on:

- the kinetic and thermodynamic parameters of the reaction (activation energy, pre-exponential factor, reaction kinetic model, reaction heat),
- the physical parameters of the material (liquid or solid states, heat capacity, thermal conductivity, density),
- and the user-controlled parameters of the experiment (such as sample size, heating rate or temperature, type of packaging, rate of heat exchange with the surroundings, gas atmosphere, etc.).

Thus, once the kinetic parameters of the reaction are known, the temperature profiles for any sample size can be accurately estimated for any desired user-controlled parameters by adequately applying the corresponding physical and thermodynamic parameters. Therefore, one can conceive the kinetic-based approach as a reasonable and possible support or alternative to the large-scale UN test H.1.

The important aspects of the kinetic workflow, i.e., the sequence of all the processes through which a kinetic analysis passes from initiation to completion, and the recommendations for proper collection of experimental data, have already been discussed in the last three ICTAC Kinetic Projects [2–4]. However, if intended for scale-up, the computational aspects of the kinetic analysis should be extended by additional recommendations about the collection of experimental data, thermodynamic and physical parameters, and the determination of the user-controlled parameters that adequately lead to the accurate determination of the heat balance. Moreover, it is necessary to quantitatively evaluate the impact of the sample mass and its physical state (liquid or solid) during: (i) experimental collection, (ii) computation of the kinetic parameters and simulation of data and (iii) prediction of reaction course and thermal hazards. In the following sections such recommendations are given. The methods of determination of SADT are illustrated by the results of evaluation of the kinetic parameters from heat flow data collected by DSC.

It is worth noting that several techniques and instruments are nowadays available for measuring the course of exothermically decomposing materials, and several laboratory practices can be found. Therefore, the legitimacy of any new evaluation method, if intended to be a reliable alternative of the large-scale UN test H.1 for accurate SADT determination, should be carefully checked for any type of investigated reactions, no matter by which technique the experimental data were collected. It is obvious that the kinetic, thermodynamic and physical parameters should be representative for the chemical reaction under investigation and that the SADT values should not be dependent on the experimental procedure used, such as real large-scales experiments, Dewar, accelerating rate calorimetry (ARC) techniques or DSC. Independently of the technique applied, the experimental data should be suitable for the computation of the kinetic parameters either in a direct way (DSC) or by simultaneously considering the results collected by two different techniques (DSC and H.1 or DSC and Dewar). This last new approach will also be explained in the following sections. The experimental data used in this study for the evaluation of SADT of azobisisobutyronitrile (AIBN) were supplied by the Federal Institute for Materials Research and Testing, Berlin, Germany, (BAM) [5]. The results obtained are compared with those presented in our previous study [6], where all experimental data for the SADT determination of AIBN were collected independently.

2. Determination of the kinetic parameters

The kinetic-based approach for the determination of SADT requires the accurate determination of the kinetic parameters which are used to numerically describe the rate and progress of the investigated reaction as a function of time and/or temperature. If the decomposition follows a single kinetic model, then the reaction can be described in terms of a single pair of Arrhenius parameters and the commonly used set of functions $f(\alpha)$ reflecting the mechanism of the process, where α expresses the reaction extent, varying between 0 and 1. The reaction rate can be described by one value of the activation energy E and one value of the pre-exponential factor A with the following expression:

$$\frac{d\alpha}{dt} = A\exp\left(-\frac{E}{RT(t)}\right)f(\alpha) \tag{1}$$

where t is time, T—temperature and R—the gas constant. Numerous sets of kinetic models are available in the literature, see e.g., Ref. [3], Farjas and Roura [7], Šimon [8] and Pérez-Maqueda et al. [9]. The truncated Šesták–Berggren (SB) model [10] can be used as a very first approximation either for single or multi-step reactions. In this second case, when the process proceeds via several sub-reactions, the general rate expression for the model containing I stages can be depicted as in Ref. [11]:

$$\frac{d\alpha}{dt} = \sum_{i=1}^{I} k_i(1-\alpha)^{n_i}\alpha^{m_i} \tag{2}$$

For example, the application of Eq. (2) for two sub-reactions by setting $m_1 = 0$ gives

$$\frac{d\alpha}{dt} = k_1(1-\alpha)^{n_1} + k_2(1-\alpha)^{n_2}\alpha^{m_2} \tag{3}$$

with the exponents n and m taken as integers and by setting $n_1 = 1$, $m_1 = 0$, $n_2 = 1$, $m_2 = 1$, the reaction rate is in this simplified case expressed as:

$$\frac{d\alpha}{dt} = k_2(1-\alpha)(Z+\alpha) \tag{4}$$

with $Z(T) = k_1(T)/k_2(T)$, the ratio of the reaction rate constants which depends on the temperature. Eq. (4) represents the reaction rate of the autocatalytic reaction built up from two sub-reactions (see Ref. [11]): (i) first order primary reaction and (ii) autocatalytic reaction. This case is similar to the approach already proposed by Kamal and Sourour [12,13] or Finke–Watzky for biological sparse data [14,15] and can be applied in two boundary situations:

- If $Z \cong 0$ (i.e., $k_1 \ll k_2$), the autocatalytic reaction is much faster than the primary reaction. The reaction rate is then expressed by the simplified equation:

$$\frac{d\alpha}{dt} \cong k_2(1-\alpha)\alpha \tag{5}$$

known as the Prout–Tompkins (PT) equation [16,17] and often used [18–23] for the description of the kinetics of autocatalytic reactions,

- If $Z \gg 0$ (i.e., $k_1 \gg k_2$), the primary decomposition determines the reaction rate which follows the first order kinetic dependence:

$$\frac{d\alpha}{dt} \cong k_1(1-\alpha) \tag{6}$$

Very often, decomposition reactions demonstrate profound multi-step characteristics and therefore do not generally obey simple rate laws. It seems obvious that there are no "true" models describing the course of the investigated reaction and therefore applied models only approximate the reality. The main question in any model-based kinetic analysis consists in finding which model would best approximate reality by the data we have recorded. Another general limitation usually arises also from the experimental procedure, when e.g., only sparse experimental data points are available [11] or when the mechanism of the reaction is not fully known as in the case of AIBN. During AIBN thermal decomposition, the cyanoisopropyl radicals produced may form via polymerization at least four products: tetramethylsuccinonitrile, methacrylonitrile, isobutyronitrile or ketenimine [24]. The mechanism is generally assumed to proceed via a homolytic scission [24,25] but it remains not fully known. When the mechanism of the decomposition of a material is complicated and not fully recognized, the isoconversional differential approach of Friedman [26] can be advantageous in the kinetic computations. Such isoconversional techniques [2,3] and evaluation methods (see e.g., Roduit [6,27–29] or software [30]) are very commonly applied in solid state kinetics for the prediction of the reaction rate and progress under any new temperature profiles. The isoconversional techniques avoid cumbersome, time- consuming and sometimes very arbitrary approaches of introducing the assumption concerning the existence of several reaction models and activation energy values necessary for the kinetic analysis of the investigated process. Because the isoconversional analysis approach does not require any knowledge of the decomposition mechanism, it avoids the risk of selecting a wrong model, which may be incorrect from a chemical point of view, which, in turn, may result in very dangerous consequences for predicting e.g., thermal aging or hazard evaluation. In isoconversional (model-free) analysis the reaction rate equation given by Eq. (7) can be used to express the rate for any temperature profile at any reaction extent α. The rate of the decomposition of AIBN for any temperature profile $T(t)$ is determined by applying the corresponding $E(\alpha)$ and $A(\alpha)f(\alpha)$ values in Eq. (7) at different degrees of conversion α.

$$\frac{d\alpha}{dt_\alpha} = A(\alpha)f(\alpha)\exp\left(-\frac{E(\alpha)}{RT_\alpha}\right) \tag{7}$$

where t_α, T_α, $E(\alpha)$ and $A(\alpha)$ are the time, temperature, apparent activation energy and pre-exponential factor, at the reaction extent α. The expression for $E(\alpha)$ and $A(\alpha)f(\alpha)$ can be obtained from the slope and the intercept with the vertical axis of the plot depicting the dependence $\ln(d\alpha/dt_\alpha)$ vs. $1/T_\alpha$. The time necessary to reach any reaction progress α is then estimated by isoconversional

kinetic predictions i.e., by the separation of the terms followed by an integration as proposed by Roduit et al. [6,27–29]:

$$t_\alpha = \int_0^{t_\alpha} dt = \int_0^\alpha \frac{d\alpha}{A(\alpha)f(\alpha)e^{-E(\alpha)/(RT_\alpha)}} \tag{8}$$

In this study, we have applied both, the "model-based" and "model-free" kinetic analyses for evaluation of the kinetic parameters required further for SADT determination of AIBN.

3. Applying the kinetic parameters and the heat balance for the scale-up

The experimental data collected in mg-scale are very often used for the evaluation of the kinetic parameters [2–4,6,27–29]. In such experiments (as e.g., DSC) experiments, the problem of the influence of the heat balance on the reaction course is generally not considered because of the small sample sizes. It is worthy to note however, that even in mg-scale for certain reaction models, e.g., for autocatalytic exothermal reactions, the amount of heat evolved during the reaction may not be completely and immediately exchanged with its surrounding, i.e., the rate of the evolved reaction heat may be greater than the rate of the heat exchanged with the environment having temperature T_e. This scenario for mg-scale has been presented recently in the third ICTAC Kinetic Project in the Section "Hazardous Materials" [4]. There we described a simple method which allows the uncovering of the possible presence of heat accumulation in the sample, increasing its temperature in an uncontrolled way and leading to the inequality $T \neq T_e$.

In the kg-scale the heat evolved during reaction cannot be instantaneously exchanged with the surroundings. The possible self-heating, leading to a temperature rise in the sample, is strongly dependent on the user-controlled parameters such as the sample mass and the physical state (liquid or solid) of the materials. In the case of self-heating, the expression for the rate of change of the sample temperature commonly applied at the mg-scale in kinetic analysis

$$\frac{dT}{dt} = \beta \tag{9}$$

with $T = T_0 + \beta t$ and $\beta \neq 0$ and $\beta = 0$ for the nonisothermal and isothermal conditions, respectively, has to be replaced by a more complicated dependence which includes the heat balance in the system required for larger sample masses. The equations of heat balance differ depending on the state of the investigated materials and are substantially different for liquids (Eq. (10)) or solids (Eqs. (12)–(14)), respectively. They are based on the theories which were initially developed by Semenov [31] for lumped systems or Frank-Kamenetskii [32] for transient heat conduction or distributed systems.

A *lumped system* is a system in which the dependent variables of interest are a function of time alone. Such a system can be represented by a uniform distribution of temperature, e.g., in liquid samples. A distributed system is a system where all dependent variables are functions of time and one or more spatial variables. Such a system has to be considered when describing the temperature gradients existing in solid samples.

3.1. Heat balance in lumped systems

The rate of the sample temperature change in classical lumped systems can be expressed, after some simplifications, by Eq. (10). The temperature of a body varies with time but remains uniform throughout at any time, $T = T(t)$. Eq. (10) describing this change

refers to Newton's law of cooling. We have:

$$\frac{dT}{dt} = \frac{US}{\rho V C_p \Phi}(T_e - T) + \frac{1}{\Phi}\frac{-\Delta H_r}{C_p}\frac{d\alpha}{dt} \tag{10}$$

where C_p, ρ, U, S, V, Φ, $-\Delta H_r$, $d\alpha/dt$ mean, respectively represent specific heat capacity, density, overall heat transfer coefficient, surface, volume, thermal inertia, specific heat of reaction and reaction rate. For lumped systems, the surface-to-volume ratio S/V can be used for the characterization of any sample container, regardless of its specific shape. The thermal inertia term in Eq. (10) (characterized by the Φ-factor) describes the heat loss and is given by

$$\Phi = \frac{mC_p + m_c C_{pc}}{mC_p} \tag{11}$$

with m and m_c representing the masses of the sample and the package, respectively. For large packages, if the lumped system assumption applies, the Φ-factor can be reasonably set to unity ($\Phi = 1$) because the mass m_c of the package is negligible compared to the sample mass m. For smaller vessels, the Φ-factor, being generally larger than one, has a direct influence on the experimental adiabatic temperature rise $\Delta T_{ad} = -\Delta H_r/(C_p\Phi)$.

3.2. Heat balance in transient heat conduction (distributed) systems

For the simulation of transient heat conduction systems, represented e.g., by the process of thermal explosion in solids, the temperature of a body, in general, varies with time as well as with spatial coordinates. In Cartesian (rectangular) coordinates, this variation is expressed as $T = T(x, y, z, t)$, where (x, y, z) indicate variation in the x-, y-, and z-axis directions, and t indicates variation with time. We can write after some simplifications

$$\frac{dT}{dt} = \frac{\lambda}{\rho Cp}\left(\frac{\partial^2 T}{\partial x^2} + \frac{\partial^2 T}{\partial y^2} + \frac{\partial^2 T}{\partial z^2}\right) + \frac{-\Delta H_r}{Cp}\frac{d\alpha}{dt} \tag{12}$$

where λ is the thermal conductivity. For the analysis of limited cylinders with given H/D ratios (H: height, D: diameter) and flat lids (e.g., drums, containers, etc.), the cylindrical coordinates are generally used and Eq. (12) can be written as

$$\frac{dT}{dt} = \frac{\lambda}{\rho C_p}\left(\frac{\partial^2 T}{\partial r^2} + \frac{1}{r}\frac{\partial T}{\partial r} + \frac{\partial^2 T}{\partial z^2}\right) + \frac{-\Delta H_r}{C_p}\frac{d\alpha}{dt} \tag{13}$$

where r represents the radius of the cylinder. Both Eqs. (12) and (13) consider the variation of temperature with time as well as position in multidimensional systems. Further simplifications of Eqs. (12) and (13) are possible if we consider the variation of temperature with time as well as position for one-dimensional heat conduction problems. In such cases, Eqs. (12) and (13) can be simplified to

$$\frac{dT}{dt} = \frac{\lambda}{\rho C_p}\left(\frac{\partial^2 T}{\partial r^2} + \frac{g}{r}\frac{\partial T}{\partial r}\right) + \frac{-\Delta H_r}{Cp}\frac{d\alpha}{dt} \tag{14}$$

in which g is a geometry factor ($g = 0$ for an infinite plate, $g = 1$ for an infinite cylinder and $g = 2$ for a sphere). In Eq. (14), the radius of the

sphere with the same volume V as the considered packaging (so-called volume equivalent sphere) can be used. We have:

$$R_{sph} = \left(\frac{3}{4\pi}V_{packaging}\right)^{\frac{1}{3}} \tag{15}$$

As illustrated in Chapter 4 for 50 kg of AIBN, such a simplification is acceptable as a first approximation for SADT determination, especially for the same overall heat transfer coefficient U and same sample masses in packages such as the cylinder with $H = D$ (i.e., $H/D = 1$) or the cube with $H = L = W$ (i.e., $H/L = 1$ and $H/W = 1$), where D, H, L and W mean the diameter, height, length and width, respectively. However, SADT values of 50 kg sample of AIBN placed in drums with H/D between 0.3 and 4 (i.e., with larger ratios of surface area per unit volume) are higher than in drums with H/D close to unity as presented later in this paper; therefore in more precise SADT simulations the real container shape has to be considered. The possible relevance of using more complex geometries (Eqs. (12) and (13)) instead of volume equivalent spheres (Eq. (14)) for SADT determination will be discussed in the following chapters. The optimal approach is generally a trade-off between efficiency and the level of required accuracy, which generally depends on several factors and changes from case to case.

3.3. Boundary conditions

Beside some simplifications introduced into Eqs. (10) and (12)–(14) and because heat passes through the package into or out of the material, from or to the surroundings three kinds of time-dependent boundary conditions are generally applied: (i) prescribed temperature at the surface (Dirichlet condition), (ii) heat flux at the surface (Neumann condition) and (iii) heat transfer at the surface (Newton law, convective heat transfer or mixed boundary conditions). For heat transfer at the surface, another frequently applied simplification considers the rate of heat conduction through the wall of the package by using the overall heat transfer coefficient U, together with the thermal resistance concept R. This concept is expressed by the equation

$$U = \frac{1}{R} \tag{16}$$

with $R = \frac{1}{h_{in}} + \sum_{i=1}^{I}\frac{d_i}{\lambda_i} + \frac{1}{h_{out}}$ (17)

where d_i represents the thickness and λ_i, the thermal conductivity of a layer i in a multilayer package with I layers constituting the wall, and h, the coefficient of heat transfer by convection inside the package (h_{in}) in case of liquid samples and at the wall surface of the package (h_{out}). The adiabatic conditions can be achieved by setting $U = 0$. The appropriate boundary conditions together with Eqs. (10) and (12)–(14) allow the self-heating of exothermally decomposed materials to be simulated after introducing the kinetic expression of the reaction rate $d\alpha/dt$ (e.g., Eqs. (1)–(7)).

Table 1
Possible physical states and temperature distribution types within the sample.

		Heat balance type	
		Distributed system with T gradients (solids)	Lumped system with T uniform (liquids)
Physical state	Solid	S & S	S & L
	Liquid	L & S	L & L

3.4. Discrimination of heat balance equations applied for SADT evaluation for liquids and solids

Because some materials can decompose in solid or liquid (after melting) states and due to the fact that we have two different types of temperature distributions within the sample (with T uniform or with T gradients), four main different cases are conceivable during SADT evaluation. They are schematically presented in Table 1.

- Case 'L & L': In this scenario, one applies the heat balance which is correct only for the liquid state and kinetic parameters evaluated from e.g., non-isothermal DSC data collected during the decomposition in the liquid state, i.e., above the melting point (ca. 100 °C for AIBN). However, due to the fact that SADT value for AIBN is lower than its melting point, this case is out of the scope of the present study.
- Case 'L & S': The situation 'L & S' corresponds to the determination of the hazard properties using the kinetic parameters calculated from the decomposition in the liquid state (above the melting temperature) together with the heat balance approach valid for the solid state. One can find a recent paper [33] where such an incorrect procedure leads to improper SADT value of AIBN which was evaluated to be in the range of 60 °C, i.e., about 10 °C higher compared to other studies [34,35]. The application of kinetic parameters characterizing decomposition in the liquid phase for the simulation of the thermal properties in the solid phase may be risky despite the application of the correct heat balance equations [6]. Therefore, using non-isothermal data of the decomposition of AIBN in the liquid state is also out of the scope of the present study.
- Case 'S & L': This case illustrates the situation in which the inappropriate heat balance equation is applied. For a 50 kg package of AIBN, the temperature distribution is not even close to being uniform, which is common for large solid samples. Despite this situation, Eq. (10), which refers to the classical lumped systems generally valid for liquids only, is sometimes used instead of Eqs. (12)–(14) for the simulation of the thermal properties of large sample in the solid state [36]. Mathematically, this approximation is used to simplify otherwise complex differential heat equations (Eqs. (12)–(14)). However, in the case of solids, the correctness of application of Eq. (10) instead of Eqs.

(12)–(14) depends in practice on the ratio of the internal and external heat flow resistances driven by the type of material and its surface area (packaging in the case of SADT), respectively. This ratio can be estimated from the Biot-number which indicates if the assumption concerning the "object temperature" at any given time assuming no spatial temperature variation within the object may be acceptable. The applicability (or inapplicability) of the classical lumped model (Eq. (10)) for SADT determination of solid materials such as AIBN will be presented later in this study in more details (Chapter 5).
- Case 'S & S': For the prediction of the hazard properties of solids that decompose already at temperatures below their melting point (such as AIBN in low temperatures applied in isothermal experiments), the correct procedure for the prediction of their SADT temperature consists in applying both, the kinetic parameters and heat balance characteristics for the solid state (Eqs. (12)–(14), Case 'S & S' in Table 1). As far as the DSC technique is concerned, the experiments for such materials should be collected isothermally in a narrow temperature window below the melting point, as recently presented by Roduit et al. for AIBN [6]. In the next chapters, this approach is applied for the isothermal DSC data, large-scale H1 tests with 5, 20 and 50 kg AIBN and Dewar data collected by BAM.

As a general rule, the correct procedure for the prediction of the thermal behavior of any material consists in applying correctly both, the kinetic parameters and heat balance characteristics for the material state.

4. Method of determination of SADT of AIBN based on DSC data (Case 'S & S', Table 1)

4.1. Recommendations for collecting proper DSC data of AIBN intended for SADT evaluation

The kinetic based method for slow cookoff and SADT determination based on few DSC signals has already been reported for some compounds elsewhere [27–28,37], and more recently also for AIBN [6]. The evaluation of the kinetics of the decomposition of energetic materials is one of the main prerequisites for the correct determination of SADT. In DSC, the most commonly applied
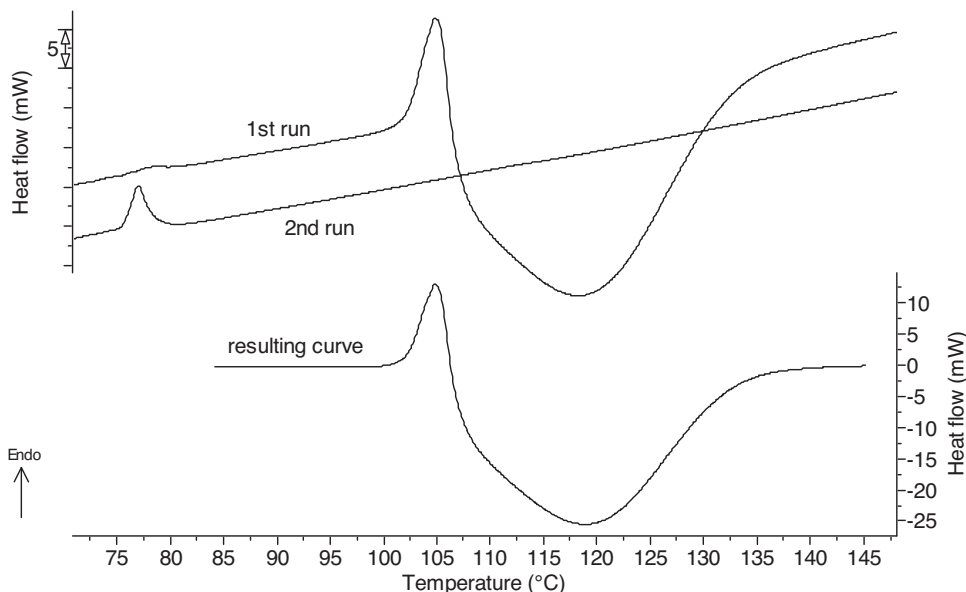

Fig. 1. Heat flow traces (*exo* down, German DIN standard) and the baseline subtracted heat flow curve of AIBN recorded by BAM by means of DSC at 5 K min⁻¹.

thermal analysis technique for examining energetic materials, the determination of the kinetic parameters from the recorded signals requires their integration in order to obtain the α-time and/or temperature relationship necessary for kinetic calculations (reaction extent α, varying between 0 and 1). The three ICTAC Kinetic Committee Projects [2–4] recommend multiple heating programs for the evaluation of reliable kinetic parameters. To fulfill this requirement, the kinetic analysis should be based on the data obtained at 4–5 different heating rates β, or at least 4–5 temperatures in isothermal conditions (or by combining both temperature programs).

However, even when applying the recommendations as presented in Refs. [2–4] for kinetic analysis, one cannot obtain a precise evaluation of SADT if these best practices are not followed by the application of proper heat balance procedures. Furthermore, sometimes data are collected under improper experimental conditions, as e.g., at too low or too high temperatures or heating rates, with too large or too small sample masses, or above melting temperature with the aim to describe the thermal behavior in the solid state. It means that some basic additional recommendations should be fulfilled prior to any kinetic analysis, in order to eliminate from the kinetic workflow the data which may be inapplicable for a given purpose or with an unacceptably low quality that could decrease the reliability of kinetic computations and lead to an incorrect scale-up.

4.2. SADT of AIBN based on non-isothermal DSC traces and heat balance appropriate for solids

BAM supplied measurements and their repetitions with heating rates of 0.5, 1, 2, 5, 10, 20 and 40 K min^{-1}, i.e., in total 14 curves. Fig. 1 reports the measurement carried out at 5 K min^{-1}.

The delivered data imply the following recommendations for SADT determination:

- For the evaluation of the kinetic parameters for materials decomposing exothermally from DSC traces, high heating rates such as 20 or 40 K min^{-1} are usually not recommended due to possible temperature gradients appearing in the samples, as reported in the last ICTAC Kinetic Project (in the chapter

dedicated to the hazardous materials [4]). Furthermore, such high heating rates are far away from the conditions of the SADT experiments, where very slow self-heating rates are present during the storage period which spans over a few days. The aim of the DSC experiments should be to best mimic and approach reaction rates as close as possible to those in the real SADT test but still in the detection range of the DSC device. The basic idea of the correct data collection consists in minimizing as much as possible the extrapolation towards the reaction rates occurring in the real packaging conditions.

- A second run with the decomposition product was performed for all heating rates. Such a second run is often used as a reference for baseline construction. However, in certain cases, as observed in supplied data, it should not be arbitrarily subtracted from the original heat flow curve because this procedure can create artefacts not observable during the real course of the reaction. For example for the traces depicted the decomposition of AIBN at 5 K min^{-1} (Fig. 1) such a subtraction in the temperature range 70–80 °C should be avoided because the "resulting curve" contains a non-existing thermal event centered at ca. 75 °C which does not appear in the fresh material (see first run in Fig. 1 and DSC curve in Ref. [6]). Due to these reasons the "resulting curve" depicted in Fig. 1 is plotted and considered only in the range 80–145 °C.

- AIBN has a melting point in the range of 100–105 °C (see Fig. 1) i.e., above SADT value of AIBN [6,34,35]. As a general rule, the kinetic parameters characterizing decomposition in the liquid phase should not be used for the simulation of the thermal properties of the solid phase, as mentioned in ICTAC Kinetics Committee Recommendations for performing kinetic computations on thermal analysis data [4], and more recently elsewhere for AIBN [6]. This situation corresponds to the previously mentioned Case 'L & S'. The evaluation of the non-isothermal measurements for AIBN may lead to an incorrect SADT determination [33] if the kinetic parameters calculated for the decomposition in the liquid phase (above melting) are applied to predict SADT in solid phase (below melting).

In summary, because they characterize the decomposition in the liquid state all non-isothermal DSC traces delivered by BAM
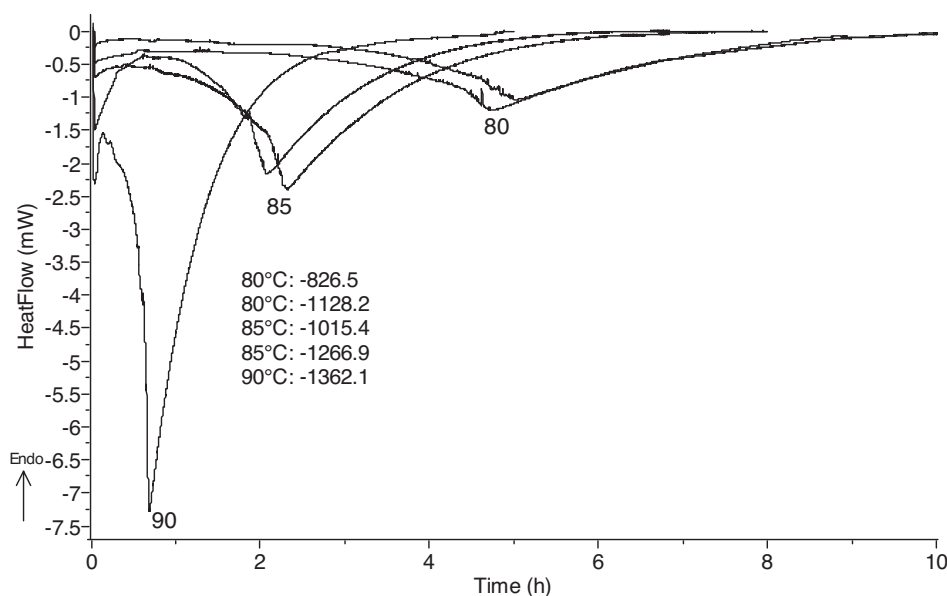

Fig. 2. BAM supplied heat flow traces of AIBN recorded by DSC (*exo* down, German DIN standard) under isothermal conditions at different temperatures as a function of time. The values of the heat of reaction (in J g^{-1}) determined at the respective temperatures are presented in the inset. The values of the temperatures in °C are marked on the curves.

have been discarded from the kinetic evaluations and have not been considered for SADT determination of AIBN in the present study.

4.3. SADT of AIBN based on isothermal DSC traces and heat balance for solids

In common practice, for the sake of minimizing the number of required experiments and limiting the workload, it is generally recommended to start the thermal analysis with a preliminary non-isothermal DSC experiment. Such a procedure allows quick uncovering of different thermal events which appear in a broad temperature range. This preliminary non-isothermal experiment with AIBN indicates that this material, existing as a solid at room temperature, is characterized by a very narrow temperature interval between melting and the beginning of the exothermal decomposition (Fig. 1). Some authors (see e.g. Ref. [36]) propose to classify such materials as quasi-autocatalytic. To fulfill the recommendations given for the Case 'S & S' (see Chapter 3.4), the kinetic analysis required for the correct SADT determination should be then performed only isothermally in the solid state, in a relatively narrow temperature window, below the melting temperature. Such a procedure for the determination of the kinetic parameters of AIBN is reported in a previous study [6], where the kinetics were investigated in the solid state in a temperature window of 78–94 °C. Similarly, BAM performed and supplied the isothermal measurements of AIBN at temperatures of 80, 85 and 90 °C. The heat flow traces after baseline subtraction (horizontal last point) are presented in Fig. 2, with their repetition at 80 and 85 °C in order to check the reproducibility of the results.

The proper collection of DSC data depends on the intrinsic properties of the reaction, as, e.g., the type of dependence of the reaction rate and/or reaction progress on time and temperature, or the kind of thermal event and amount of heat released (consumed). This can significantly influence the choice of sample mass and the optimal temperature window in isothermal or non-isothermal experiments. In view of choosing an adequate temperature range, the criterion of minimal acceptable signal intensity for the lowest temperature in the case of isothermal experiments depends also on experimental limitations such as the maximal mass which can be placed in the crucible (lower border of the experimental window). Considering the DSC technique as an example and assuming a sample mass of 10 mg and a minimal sensitivity of the DSC sensor of 10 μW, the minimal intensity of the recorded signal should be ca. 100 times larger, i.e., in the range of about 1 mW. Sufficient heat flow intensity is reached for AIBN with sample masses of ca. 14–15 mg at a temperature of 80 °C or above, as presented in Fig. 2. This result is in line with those presented in Ref. [6], where, for similar sample masses of 14 mg, maximal values of the heat flow in the range of ca. 1 mW were recorded for AIBN at 78 °C. In the experiments carried out at lower temperatures, the signal-to-noise ratio was too low. Application of such results in kinetic analysis may be problematic due to the difficulties in the correct construction of the baseline and determination of the α-time dependence. The choice of the lowest experimental temperature (and/or heating rate) in combination with the sample mass is additionally dependent on the sensitivity and specific construction characteristics of the thermoanalyzer. A DSC 1 (Mettler Toledo) was applied in our study [6], whereas a Pyris (PerkinElmer) device was used by BAM.

One can observe large variations of the values of the heat of reaction determined from DSC traces supplied by BAM (Fig. 2), which vary between −826.5 J g⁻¹ and −1362.1 J g⁻¹ (difference of 535.6 J g⁻¹). Furthermore, considering all BAM data measured under isothermal conditions, the mean value of ΔH_r amounts to -1119.82 J g⁻¹ with a standard deviation of 210.6 J g⁻¹ (ca. 18.8%).

This mean value of the heat of reaction ΔH_r is significantly smaller than the one reported in our previous study [6] which amounted to −1477 J g⁻¹, with a much smaller standard deviation in the range of ca. 5%. The heat of decomposition determined in Ref. [6] is much closer to the values reported by other authors (ΔH_r = −1401 J g⁻¹ [38,39]) or determined in experiments performed with static bomb calorimetry (ΔH_r = −1498 J g⁻¹ [40] and −1394 J g⁻¹ [41]). The observed deviations in the mean value of ΔH_r evaluated from the DSC data supplied by BAM indicate that an optimization of the experimental procedure may result in a possible increase of their accuracy. The valuable recommendations concerning the proper collection of thermoanalytical data used for kinetic analysis given in Ref. [4] may help to significantly improve their quality.

The kinetic parameters were computed by both "model-based" and "model-free" kinetic analyses. Due to the observable induction period followed by an accelerating and decelerating reaction rate under isothermal conditions (see Fig. 2) which is typical for autocatalytic reaction, the Kamal–Sourour (KS) model (Eq. (4)) has been taken for further considerations for the "model-based" kinetic analysis. The kinetic parameters with fitted (Eq. (3)) and fixed exponents taken as integers (Eq. (4)) evaluated by AKTS-Thermokinetics software [30] are reported in Table 2. The other typical autocatalytic PT-model (Eq. (5)) was not taken into consideration due to worse fit of the measured data. It seems questionable whether complicated set of reaction stages including numerous combinations of consecutive and parallel stages can fully mimic the very complicated course of the AIBN decomposition with several elementary (usually unknown) processes taking place simultaneously. Designing more and more complicated reactions schemes and trying to include too many steps into considerations we can easily reach the stage in which proposed scheme is far away from the reality. Therefore, according to the Ockham's razor principle of simplicity, we applied only the autocatalytic approach expressed by Kamal–Sourour (KS) equations in order to include into kinetic workflow the correct description of the S-shaped autocatalytic dependence alpha-time observable under isothermal conditions. Results of this procedure are satisfactory despite the fact that applied KS equation can be treated only as the mathematical, simplified mechanistic representation of the reaction.

For the "model-free" computations, the differential isoconversional kinetic analysis (see Eq. (7)) has been applied. The results are presented in Fig. 3A in the form of a relationship between the apparent pre-exponential factor and the activation energy vs. the reaction progress α. Comparison of the simulated and experimental reaction progresses in mg-scale derived from the kinetic parameters evaluated by isoconversional (model-free) and model-based approaches is presented in Fig. 3B. The poor reproducibility of the experimental data does not allow the precise fit between the simulated and experimental traces, however, the fit achieved by isoconversional analysis seems to better mimic the reaction course.

Table 2
Kinetic parameters calculated by non-linear regression applying a two-step reaction model where the autocatalytic reaction is built up from two sub-reactions (KS-model) (Eqs. (3) and (4)). Kinetic parameters were evaluated for fitted or fixed exponents (n,m) in the KS equation.

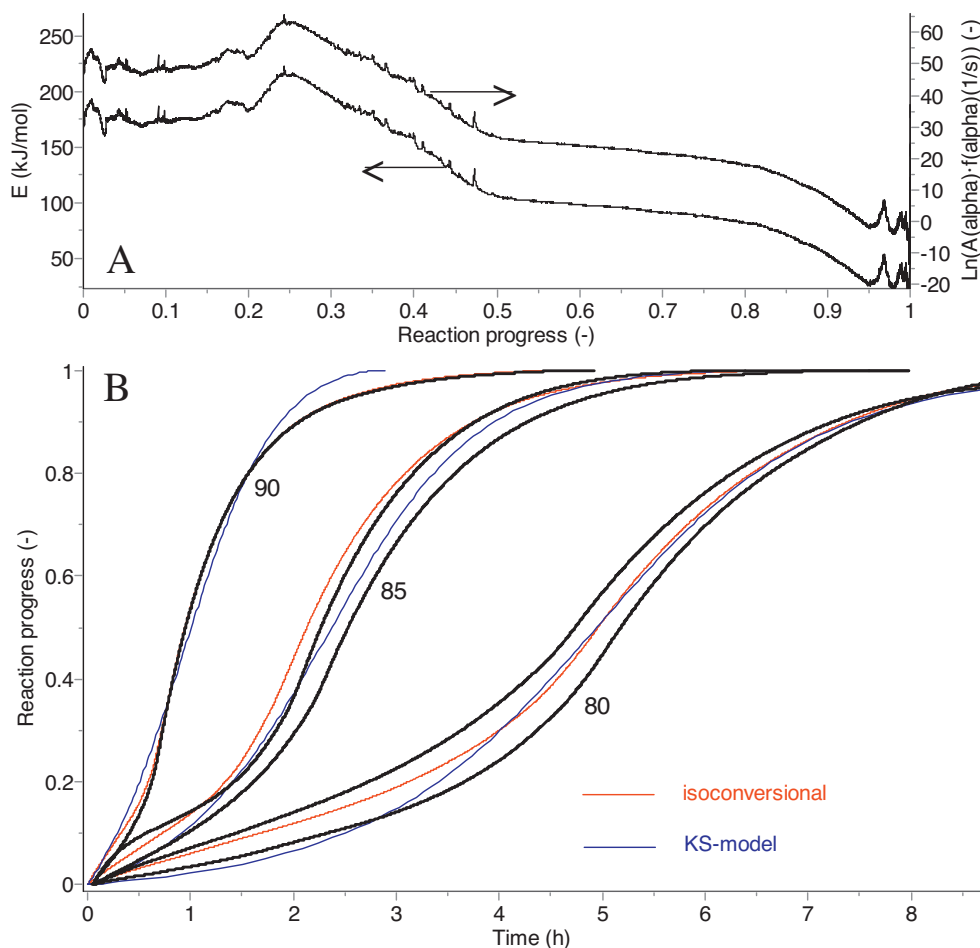|	KS-model (n, m) fitted	KS-model (n, m) fixed
A_1 (s⁻¹)	1.83E + 39	1.97E + 44
E_1 (kJ mol⁻¹)	301.3	336.7
n_1 (−)	0.417	1
A_2 (s⁻¹)	3.68E + 06	1.16E + 09
E_2 (kJ mol⁻¹)	68.3	85.7
n_2 (−)	1.129	1
m_2 (−)	1.164	1

Fig. 3. Results of the differential isoconversional kinetic analysis of AIBN decomposition in the solid state based on the DSC signals recorded isothermally. (A) Activation energy $E(\alpha)$ and $A(\alpha)f(\alpha)$ as a function of the reaction progress. (B) Comparison of the experimental (black) and simulated reaction progresses in mg-scale in isothermal temperature mode calculated using kinetic parameters obtained by "model-based" (blue) and "model free" (differential isoconversional) (red) kinetic analyses, respectively. The values of the temperatures in °C are marked on the curves.

The reaction rate and progress can be predicted also in the kg-scale by combining the reaction rate evaluated by the autocatalytic model (Eq. (3)) and differential isoconversional analysis (Eq. (7)) with the appropriate heat balance equation depicting the temperature evolution in the sample given by dT/dt values (Eqs. (12)–(14)) in the solid material. In the present study, the SADT values evaluated in simulations are expressed by numbers containing two digits after the decimal point. Such a precise evaluation helps to better illustrate the influence of the considered parameters on the simulation results. In practical applications, all precise simulated values have to be transformed to the final SADT values according to the UN recommendations [1] in which the SADT is the critical ambient temperature (°C) rounded to the next higher multiple of 5 °C.

The values of physical parameters of AIBN required for SADT determination were supplied by BAM and amount to: $C_p = 1.55 \, \mathrm{J\,g^{-1}\,K^{-1}}$ and $\lambda = 0.127 \, \mathrm{W\,m^{-1}\,K^{-1}}$. Besides the isothermal DSC experiments, BAM also performed the UN SADT test H.1 with sample masses of AIBN of 5, 20 and 50 kg, respectively. In these experiments, the shape and size of the vessels were the following:

(i) 5 kg test: Fibreboard box (4G) thickness about 5 mm, length $L = 39$ cm, width $W = 39$ cm, height $H = 35$ cm. Substance in plastic foil (<0.1 mm). Filling height about 16 cm but the

substance does not cover the whole ground area (about 29×22 cm covered).

(ii) 20 kg test: Fibreboard box (4G) thickness about 5 mm, length $L = 39$ cm, width $W = 29$ cm, height $H = 46$ cm. Substance in plastic foil (<0.1 mm). Filling height about 26 cm.

(iii) 50 kg test: fibre drum (1G) thickness about 5 mm, removable head made from wood about 7 mm, diameter $D = 46$ cm, height $H = 63$ cm. Substance in plastic foil (<0.1 mm), filling height about 46 cm.

The filling volumes in these large-scale tests amounted to ca. 76.4, 29.4 and 10.2 L for sample masses of 50, 20.25 and 5.05 kg, respectively. These volumes have been used in our calculations for the determination of bulk density required for SADT determination.

Because in the strict sense the mechanism of AIBN decomposition in solid phase is not fully known (see Chapter 2) our simulations presented below are based on the kinetic parameters evaluated by the differential isoconversional kinetic analysis which does not require any knowledge of the decomposition mechanism. The value of a heat transfer coefficient U in the first approximation was based on the UN Recommendations [1] and the claims found in the paper published by BAM [42] in which in the large-scale experiments the U value is considered in the range between 4 and $8 \, \mathrm{W\,m^{-2}\,K^{-1}}$. To evaluate more precisely this value from the

experimental data we used the dependence temperature-time supplied by BAM presented in Chapters 4 and 6. The U value was evaluated from the initial part of the dependence T–t, i.e., in the period in which the material can be treated as inert (time between 0 and ca. 3 days in which the amount of the evolved heat due to AIBN decomposition is negligible). The best fit was obtained for the U value amounted to 4.9 W m^{-2} K^{-1} which was afterward used in all our simulations. The computed SADT amounts to 47.16 °C (see Fig. 4). For the simulation, a limited cylinder with flat lids has been used with the same ratio $H/D = 1$ corresponding to the large size 50 kg H.1-test used by BAM (filling height $H = 46$ cm and $D = 46$ cm). Fig. 4 presents the surrounding temperature corresponding to SADT and the evolution of other temperatures inside the drum at specific locations namely at its center ($R = 0$; $H/2$), at position ($R/2$; $H/4$) and at its surface (R; $H/2$) vs. time (with $R = D/2$). The average reaction progress α vs. time is presented at the bottom of Fig. 4.

Our simulations based on kinetic parameters evaluated from DSC signals and the correct heat balance in the system indicate that a temperature of 47.16 °C is the lowest environment temperature at which overheat in the middle of considered 50-kg packaging exceeds 6 °C ($\Delta T6$) after a lapse of seven days (168 h) or less. This period is measured from the time when the packaging center temperature reaches 2 °C below the surrounding temperature (after ca. 2.02 days) (Point A). After about 2.44 days (Point B) the center temperature is equal to the surrounding temperature. The overheat of 6 °C occurs after about 9.02 days (Point C). At this time the average reaction progress in the 50 kg package amounts to ca. 0.03 (3%) (bottom, right axis).

Fig. 5 presents the calculated spatial distribution of the temperatures (left column) and reaction progresses (right column) in the drum after lapse of time represented by the points A, B and C i.e., when the center temperature differs by −2 °C, 0 °C and +6 °C, respectively compared to the surrounding temperature. The yellow circles in Fig. 5 display the spatial positions of the temperature measuring points, namely: $T7$ (at the center, $R = 0$; $H/2$), $T2$ ($R/2$; $H/4$) and $T4$ (close to the surface, R; $H/2$).

The validation of the computed SADT value can be performed by comparing the simulated SADT with the results of the experiment performed by BAM with a 50 kg package of AIBN exposed to a surrounding temperature of 47 °C until runaway (Fig. 6). From this experiment, following the UN test H.1 procedure, BAM determines SADT of a 50 kg package of AIBN as equal to 47 °C. Temperatures inside the sample were measured at the following positions in the drum: $T1$ (R; $H/4$), $T2$ ($R/2$; $H/4$), $T3$ ($R/2$; $H/2$), $T4$ (R; $H/2$), $T5$ (surface), $T6$ ($R/2$; $3H/4$), $T7$ (center) ($R = 0$; $H/2$), $T8$ (surroundings). For the sake of clarity, Fig. 6 presents only the temperature evolution at points $T7$ ($R = 0$; $H/2$) at center, $T2$ ($R/2$; $H/4$) and $T4$ (R; $H/2$) which correspond to the spatial positions depicted by the yellow circles used in our simulations (see text above and Fig. 5). A rapid temperature rise (corresponding to a thermal runaway) in BAM experiment was observed after 10.2 days. When comparing the time to runaway values it is necessary to remember that our simulations presented in Fig. 7A show that the change of the surrounding temperature by only one degree, from e.g., 48 to 49 °C, results in decreasing the time to runaway for ca. 3 days (from ca. 9 to 6 days).

Further simulations of T–t dependences and runaway scenarios are presented in Fig. 7A–C for sample masses of 50 kg (drum, $H = D = 46$ cm), 20 kg (box, 39 cm × 29 cm × 26 cm) and 5 kg (box, 29 cm × 22 cm × 16 cm), respectively. In all figures, the bold curves represent the temperatures at the center which, based on the definition of the UN H.1 test, correspond to SADT, i.e., 47.16, 49.86 and 54.77 °C for sample masses of 50, 20 and 5 kg, respectively. The additional lines in all figures present the center temperature profiles for other external temperatures T_e below and above SADT, i.e., in Fig. 7A between 45 and 50 °C (i.e., from SADT −2 °C to SADT +3 °C) and in Figs. 7B and C from SADT −1 °C to SADT +1 °C.

The SADT values of AIBN obtained in these simulations are in line with the SADT values already reported in other studies [6,34,35]. Computed SADT values are additionally in very good agreement with the results of three large-scale H.1-tests performed by BAM with reported SADT of 47 °C (see Fig. 6), 48 °C and >49 °C for 50, 20 and 5 kg, respectively (in this last experiment BAM performed two tests at 47 and 49 °C, however the SADT criterion was not fulfilled at these temperatures).
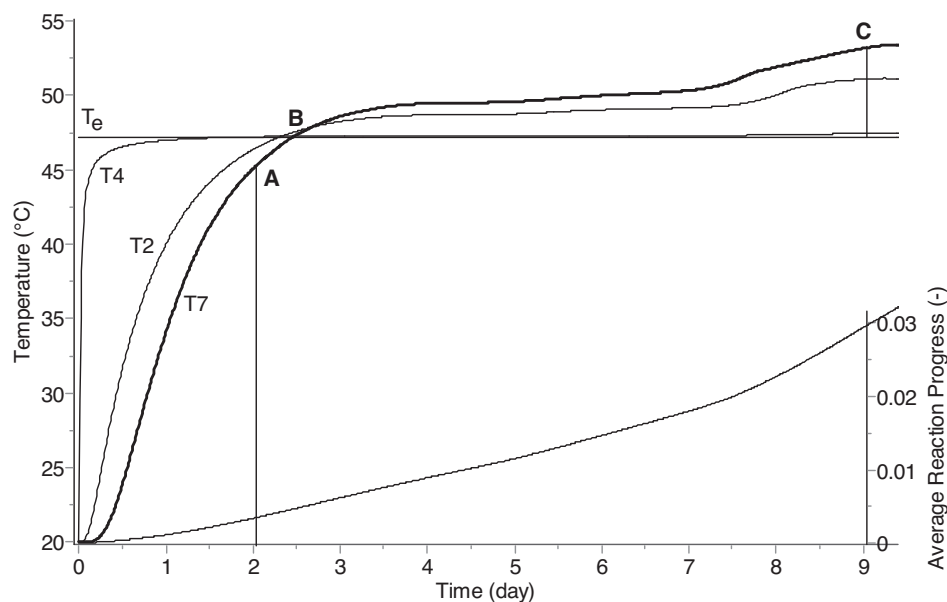

Fig. 4. Simulation of the SADT for 50 kg of AIBN in a drum with filling height $H = 46$ cm and $D = 46$ cm. Our simulated SADT value according to the definition of the SADT (Test H.1) [1] amounts to 47.16 °C. Point (A) indicates the time when the packaging center temperature (bold) reaches 2 °C below the surrounding temperature. At point (B) the sample reaches the surrounding temperature. The overheat of 6 °C occurs after about 9.02 days (point C). At this time the average reaction progress of AIBN decomposition in the 50 kg package amounts to ca. 0.03 (3%) (bottom, right axis). The curves labelled as $T7$, $T2$ and $T4$ represent the temperature of AIBN at the following spatial positions: $T7$ ($R = 0$; $H/2$), $T2$ ($R/2$; $H/4$) and $T4$ (R; $H/2$).
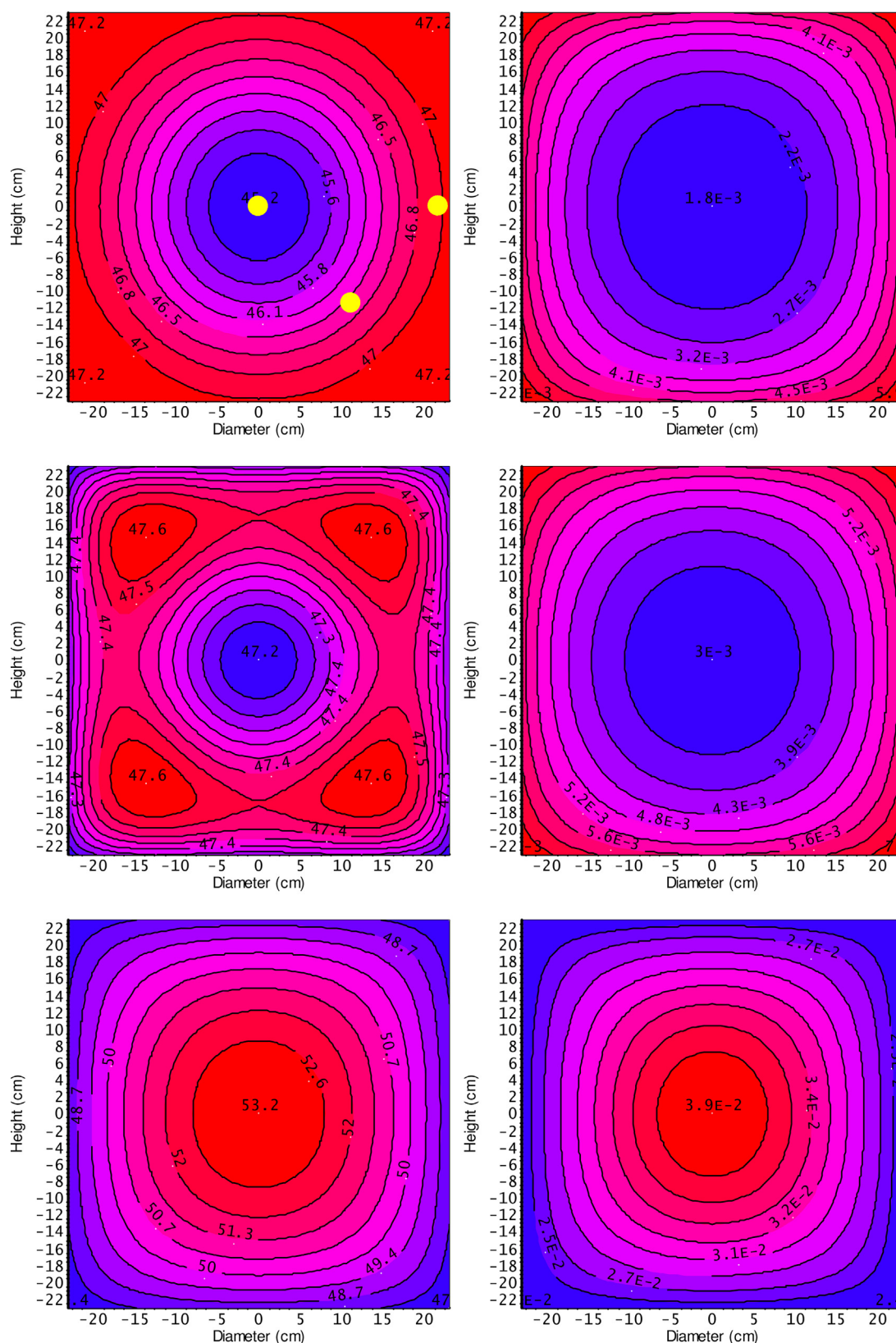
Fig. 5. Simulations of the spatial distribution of AIBN temperature (left) and reaction progress α (right column) for a mass of 50 kg in a drum with ratio H/D = 1 after periods of time represented by the points A (top), B (middle) and C (bottom) depicted in Fig. 4. Positions of points T7, T2 and T4 (in this order from left to right) are marked by yellow circles in the upper-left plot.

Finally, the computed SADT values with the "model-based" approach (Eq. (3), Table 2) also fit the experimental values well as depicted in Table 3 summarizing all experimental (BAM) and simulated (AKTS) SADT values.
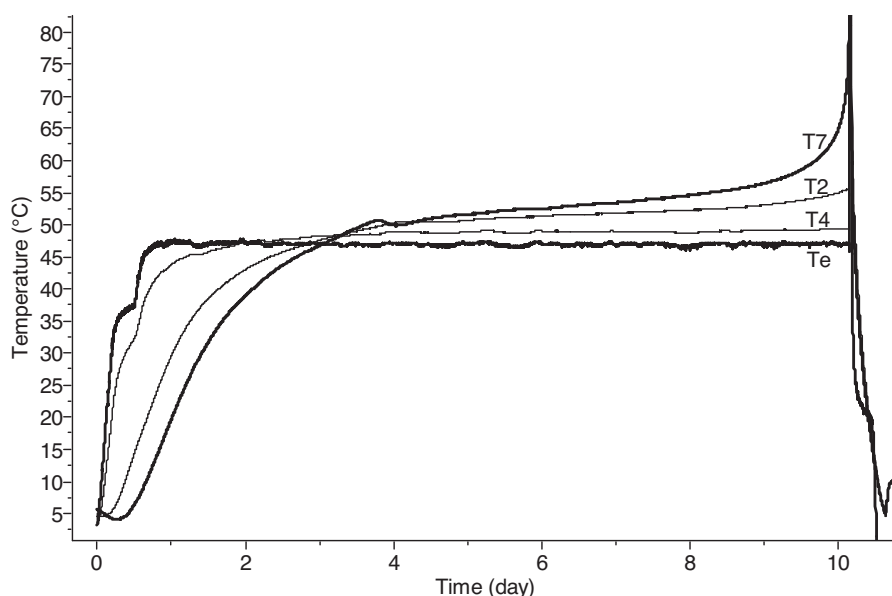
Fig. 6. Temperature-time dependence monitored experimentally during UN SADT test H.1 of 50 kg of AIBN performed by BAM in a drum with filling height $H = 46$ cm and $D = 46$ cm. SADT amounts to 47 °C. The curves represent the temperature of AIBN at following spatial positions: $T7$ ($R = 0$; $H/2$), $T2$ ($R/2$; $H/4$) and $T4$ (R; $H/2$). A rapid temperature rise corresponding to a thermal runaway was observed after 10.2 days.

4.4. Influence of the package shape, sample mass m and overall heat transfer coefficient U on the SADT values

The influence of the shape and size of the package containing $m = 50$ kg for $U = 4.9$ W m^{-2} K^{-1} on SADT value has been observed in simulations; however it is rather negligible. The samples packed in a cubic box (42.4 cm × 42.4 cm × 42.4 cm) (Eq. (12)) and in volume equivalent sphere ($R = 26.3$ cm) (Eqs. (14) and (15)) have SADT values which amount to 47.36 and 46.99 °C, respectively. The sphere-shape package leads to the most conservative result because its surface to volume S/V ratio is minimal. The influence of S/V ratios on the SADT is presented in Fig. 8 for a fixed mass of AIBN (50 kg) and different shapes of drums with various H/D ratios (in the range of 0.3–4). The simulated results indicate that the SADT values of AIBN with the constant mass do not significantly depend on the considered container shapes. Because in practice the SADT values are rounded to the next higher multiple of 5 °C [1], observed differences support the use of a spherical shape in the first approximation of SADT determination.

The computed SADT values of AIBN for different combinations of the sample mass m and overall heat transfer coefficient U based on the definition of the H.1-test recommended by the United Nations [1] are reported in Table 4. For SADT determination and the computations, limited cylinders of different sizes have been used with flat lids and the same ratio $H/D = 1$ (filling height $H = 46$ cm and $D = 46$ cm) as those used by BAM for its large size 50 kg H.1-test.

5. Influence of the cooling coefficient evaluation method on scale-up of H.4 test based on thermal equivalence approach (Case 'S & L')

The results presented in previous chapters indicate that the correct heat balance of the investigated system is the very important prerequisite for the correct scale-up procedure when thermal behavior in the kg-scale is predicted from the results collected in the mg-scale. However, this problem is also of great importance when a scale-up is carried out during increasing sample mass only by two orders of magnitude as it occurs when applying the Dewar H.4 test for the evaluation of SADT for 50 kg

samples. Applying the results of the H.4 test in order to mimic the results of the H.1 test one has to choose the correct method of evaluation of heat loss per unit mass value which has to be in the Dewar H.4 test similar to those in the package offered for transport.

The H.1 test is designed for testing real packages up to 220 liters. As a smaller-scale test for SADT determination, one can consider the H.4 test as described in details in the UN Manual [1]. Because this test is carried out at a laboratory-scale, scale-up to the real size of packages is necessary. The UN Manual recommends in scale-up procedures the concept of the heat loss similarity in which the heat loss per unit of mass in the small-scale test should be similar to that in the real size package. The concept is derived from Eq. (10) where the main resistance to heat flow is considered to be at the package walls (low viscous liquids, lumped systems). According to this approach the container filled with a liquid material has a similar thermal behavior as a Dewar if their heat loss characteristics are similar. If the system is inert or at the temperatures at which the reaction rate is insignificant, for the same material, or for materials having similar physical properties, we obtain from Eq. (10):

$$\frac{U_1 S_1}{m_1 \Phi_1} = \frac{U_2 S_2}{m_2 \Phi_2} \tag{18}$$

with indices 1 and 2 representing the large size container and the Dewar, respectively, and m, U, S and Φ representing the mass of material, overall heat transfer coefficient, surface and thermal inertia, respectively. In the UN Manual the thermal inertia factor of the Dewar is neglected and Eq. (18) is simplified to

$$\frac{U_1 S_1}{m_1} = \frac{U_2 S_2}{m_2} \tag{19}$$

However, in the strict sense, the Φ-factor can be set to unity for large packages only. Assuming $\Phi = 1$ and considering the sample mass $m = \rho V$, constant external temperature T_e and negligible reaction rate, Eq. (10) can be expressed in the form
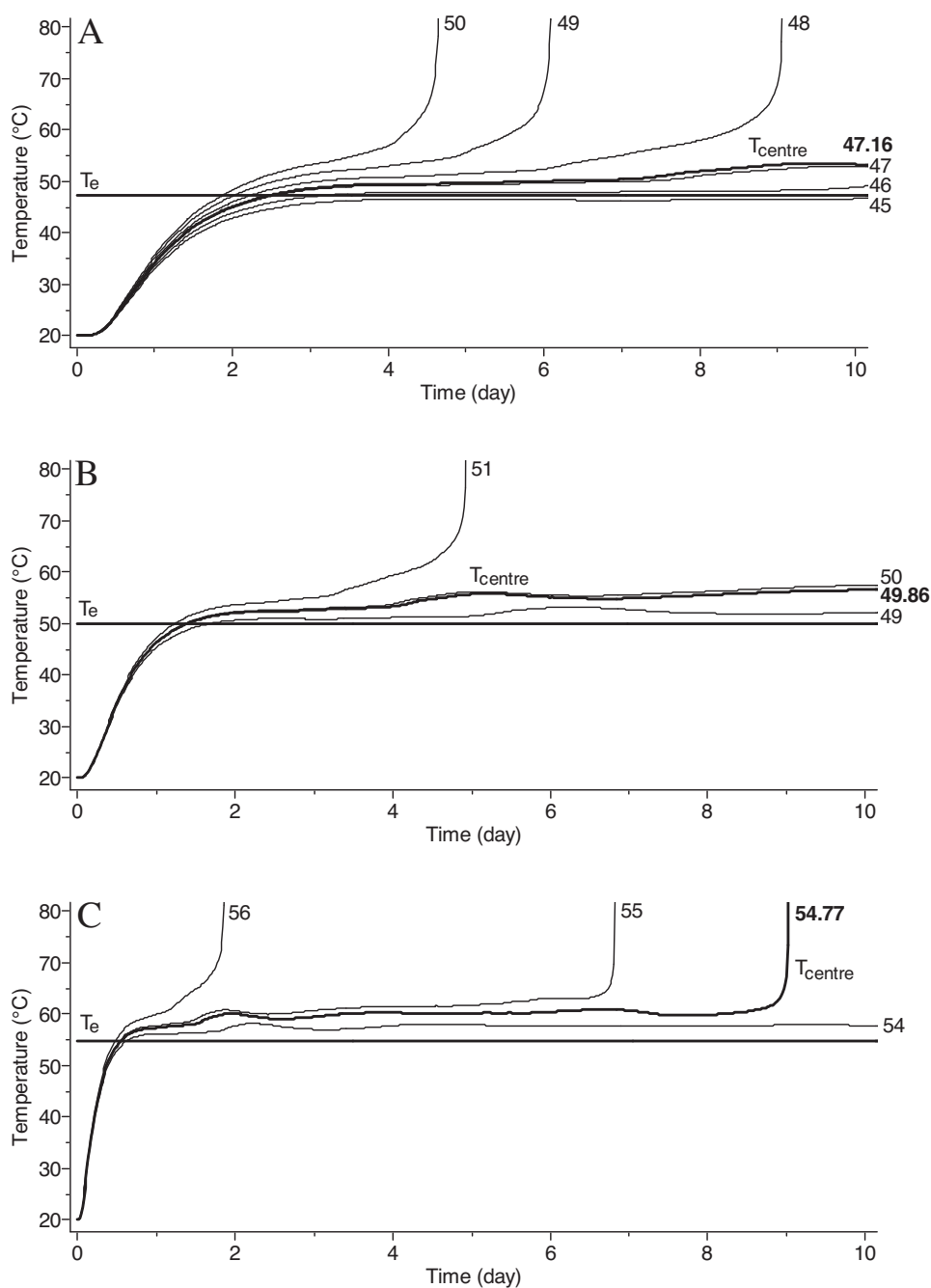
Fig. 7. Simulated temperatures in center of AIBN samples for the masses of (A) drum, 50 kg, (B) box, 20 kg and (C) box, 5 kg, with λ = 0.127 W m⁻¹ K⁻¹ and U = 4.9 W m⁻² K⁻¹, respectively. Temperatures of SADT are marked in bold. The exact dimensions of the drum and boxes and other parameters used for the simulations are given in the text.

Table 3
Summary of the experimental (BAM) and simulated (AKTS) SADT values of AIBN. Simulations were based either on the "model-based" or "model-free" (differential isoconversional) kinetic analyses, experiments were carried out according to the UN SADT tests H.1 [1] procedure. Evaluations were done for a limited cylinder with flat lids for the 50 kg and for boxes for the 20 and 5 kg of AIBN, respectively. Other parameters used for the simulation are given in the text.

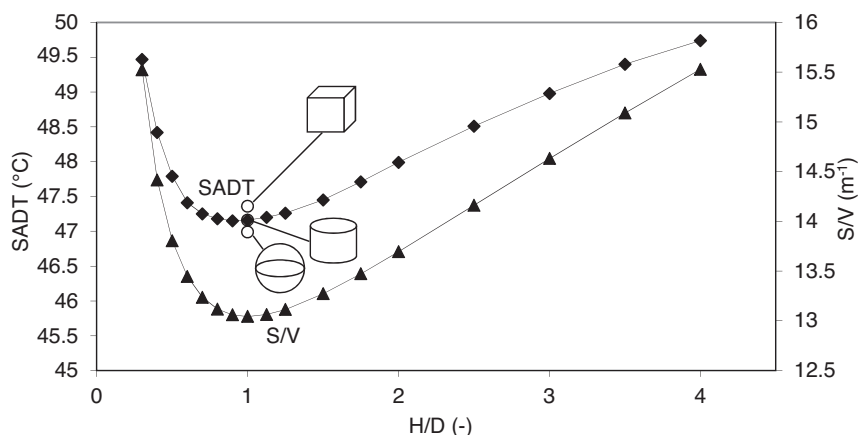|	SADT (50 kg drum)	SADT (20 kg box)	SADT (5 kg box)
Isoconversional (Eq. (7), Fig. 3A)	47.16 °C	49.86 °C	54.77 °C
KS-model (n, m fitted Eq. (3), Table 2)	48.74 °C	49.19 °C	49.72 °C
UN test H.1 (BAM)	47 °C	48 °C	>49 °C

Fig. 8. SADT (left) and S/V ratios (right axis) of 50 kg sample of AIBN placed in drums with H/D between 0.3 and 4. SADT is higher for drums with larger ratios of surface area per unit volume. Parameters used for the SADT determination are given in the text. The SADT values for other container shapes with the same sample mass (cube and sphere) and $U = 4.9$ W m^{-1} K^{-1} are additionally presented in the plot. For the cube, cylinder with $H/D = 1$ and sphere SADT values amount to 47.36 °C, 47.16 °C and 46.99 °C, respectively.

Table 4
Dependence of the SADT (°C) for AIBN on the overall heat transfer coefficient U (W m^{-2} K^{-1}) and the sample mass m expressed in kg evaluated by kinetic-based simulations (differential isoconversional analysis, Eq. (7)). Evaluations were done for limited cylinders with flat lids and ratio $H/D = 1$ (Eq. (13)). For sample masses of 50, 20 and 5 kg with $U = 5$ W m^{-1} K^{-1} SADT values amount to 47.17, 49.57 and 53.68 °C, respectively. Verification of these values by large scale UN SADT tests H.1 is given in the text.

		Sample mass m (kg)								
		250	100	50	20	10	5	0.5	0.25	0.1
Overall heat transfer coefficient U/W m^{-2} K^{-1}	10	44.79	46.2	47.54	49.91	52.48	54.56	58.77	59.38	59.94
	5	44.66	46	47.17	49.57	51.71	53.68	58.18	58.87	59.51
	2	44.34	45.53	46.52	48.22	50.07	51.56	56.51	57.45	58.34
	1	43.98	45.04	45.79	46.82	48.14	49.59	53.81	54.92	56.46
	0.5	43.74	44.46	45.08	45.81	46.43	47.11	50.65	51.89	53.42
	0.4	43.71	44.31	44.85	45.53	46.06	46.6	49.85	50.79	52.41
	0.3	43.73	44.17	44.58	45.18	45.65	46.1	48.79	49.71	50.98
	0.2	43.84	44.1	44.35	44.74	45.12	45.51	47.11	48.08	49.39
	0.1	44.07	44.19	44.28	44.42	44.54	44.73	45.74	46.11	46.74
	0.05	44.11	44.3	44.36	44.4	44.43	44.47	44.87	45.12	45.53

$$\frac{\mathrm{d}T}{T - T_e} = -\frac{US}{mC_p}\mathrm{d}t \qquad (20)$$

After integration of Eq. (20) from $t = 0$ to time t, i.e., from the initial temperature $T = T_0$ to $T = T(t)$ we obtain:

$$T = T_e + (T_0 - T_e)\exp\left(-\frac{1}{\tau}t\right) \qquad (21)$$

and

$$\ln\left(\frac{T - T_e}{T_0 - T_e}\right) = -\frac{1}{\tau}t \qquad (22)$$

with τ being the so-called time constant and the term $1/\tau$ with dimension (time)$^{-1}$ representing the cooling coefficient of the material. Eq. (22) is used in the method reported in the UN Manual (Section 28.3.6 in Ref. [1]) based on a continuous monitoring temperature of the substance $T(t)$ and surroundings T_e which allows the calculation of the term $1/\tau$ by linear regression in a semi-log plot of the fractional unaccomplished temperature difference vs. time (further labeled as FUTD in this study).

In the UN Manual, it is further proposed for determining the thermal equivalence of cooling characteristics for packages of various shapes and sizes (see Sections 28.3.5 and 28.3.6 in Ref. [1], respectively) to compute the heat loss per unit of mass (usually given in W kg^{-1} K^{-1}) which can be estimated using the following dependence:

$$L = \frac{1}{\tau}C_p \qquad (23)$$

Alternatively, it is proposed (Section 28.3.5 in Ref. [1]) to derive the heat loss L (W kg^{-1} K^{-1}) by considering specific heat of the substance and the half-time of cooling $t_{1/2}$ (further named as "Half-Cooling Time" and labelled as HCT in this study). By setting $T(t_{1/2}) = T_0 + (T_e - T_0)/2$ in Eq. (22), one obtains the following relationship for the calculation of the cooling coefficient

$$\frac{1}{\tau} = \frac{\ln(2)}{t_{1/2}} \qquad (24)$$

and after combining Eqs. (23) and (24), the heat loss from the half-cooling time reads:

$$L = \frac{\ln(2)}{t_{1/2}}C_p \qquad (25)$$

Thus, in the UN Manual, two methods for scale-up based on the thermal equivalence of packages of different shapes and sizes are proposed. The difference between them lies in the way of calculating the cooling coefficient, which can be obtained experimentally either by the FUTD- or the HCT- methods, respectively.

According to the UN Manual the above presented concept of scale-up can be applied to liquids and solids in the case of the UN test H.4 performed with Dewar vessel. This issue has been widely

debated in the literature when applied to solid materials, see e.g., Refs. [34,42–44].

After setting the reaction rate dα/dt = 0 for inert systems, the sample temperature $T = T(t)$ in lumped system (Eq. (10)) or the temperatures at any position $T = T(x, y, z, t)$ in distributed system, (Eqs. (12)–(14)) can be computed for any surrounding temperature and package shape, size and filling degree. The prerequisite for the application of Eqs. (10), (12), (13) or (14) is the knowledge of both, the internal and external heat transfers. They are derived, on the one hand, from the physical properties of a substance and, on the other hand, from the heat transfer through the package considering the convection at its surface typical for transport and storage. The rate of cooling calculated this way takes into account "the quantity of substance, dimensions of the package, heat transfer in the substance and the heat transfer through the packaging to the environment", which fulfills the recommendations required in the UN Manual (Section 28.3.5 in Ref. [1]) for scale-up applying the concept of thermal equivalence.

Because in the calculations based on the UN Manual the values of the heat loss per unit mass are generally reported in the form of a product of the cooling coefficient $1/\tau$ by the specific heat capacity of the sample C_p in Table 5 we also present these values (rounded to unity for better clarity) expressed in mW kg^{-1} K^{-1}. Table 5 includes the data for two sample masses of AIBN: 50 kg and 285 g which were used in the tests performed by BAM, namely UN H.1 and H.4, respectively. In Fig. 9, the temperature evolution in the material in the center ($R = 0$; $H/2$) (labeled as A) and in the position ($R/2$; $H/4$) (labeled as B) are simulated for the sample mass $m = 50$ kg of AIBN with $U = 4.9$ W m^{-2} K^{-1} (see also Figs. 4 and 5). Before the center temperature reaches 2 °C below SADT the heat generated by the reaction is small and temperature-time dependence for AIBN is almost like for an inert material. In Fig. 9, the influence of the reaction heat on the temperature-time dependence is represented by the bold and thin curves for the cases when the heat generated by the reaction is considered (bold) or neglected. An initial lag of the temperature is observable especially at the sample center in distributed systems. During the evaluation of the cooling

coefficient, this time lag may be considered or ignored which, in turn, may have some influence on the heat loss values depicted in Table 5. It is generally recommended to ignore this time lag which corresponds to the point when the slope of the logarithm of the fractional unaccomplished temperature difference vs. time becomes constant (see Fig. 9, bottom). According to this recommendation, the determination of the characteristic cooling rate of the system by the FUTD-method is based on the slope of parallel lines in Fig. 9 (bottom). A cooling coefficient, characterizing the cooling rate of the system, determined in such a way, is independent of the position of the thermocouple in the material during an experiment. On the contrary, if the cooling coefficient is determined by the HCT-method in the distributed systems, its value depends on the position of the thermocouples inside the material, which leads to greater deviations (see the coordinates ($t_{1/2}$, 33.5 °C) in Fig. 9, top). Furthermore, the accuracy of the determination of the cooling rate is also reduced if performed at surrounding temperatures close to SADT, when the heat production is noticeable (bold lines in Fig. 9). Simulation results presented in Fig. 9 indicate that the determination of the cooling coefficient should be preferably performed: (i) with experiments at surrounding temperatures much below SADT when the thermal characteristics of the materials are much closer to those of an inert substance and (ii) by the FUTD-method considering the period after the time lag when the cooling coefficient is independent of the position of the temperature sensors in the material.

The heat loss values calculated from Eqs. (22) and (23) with the FUTD-method for both sample masses are presented in Table 5. The table depicts the heat loss values for cases with and without considering the time lag, and without considering both, the time lag and the heat released by the reaction (thin line in Fig. 9). Additionally, the table depicts the heat loss values calculated by the HCT-method. For every SADT value, the upper and lower lines in respective rows indicate the calculated heat loss at the center ($R = 0$; $H/2$) and at the position ($R/2$; $H/4$). For the simulation we have applied the same ratio $H/D = 1$ as those in the large size 50 kg H.1-test performed by BAM.

Table 5
Dependence of SADT and heat loss (W kg^{-1} K^{-1}) calculated by different methods on the overall heat transfer coefficient U (W m^{-2} K^{-1}) and the amount of AIBN expressed in kg. The calculations were performed for cylinders with the ratio $H/D = 1$. For every SADT value, the upper and lower lines in respective rows indicate the calculated heat loss in the sample center ($R = 0$; $H/2$) and in the position ($R/2$; $H/4$).

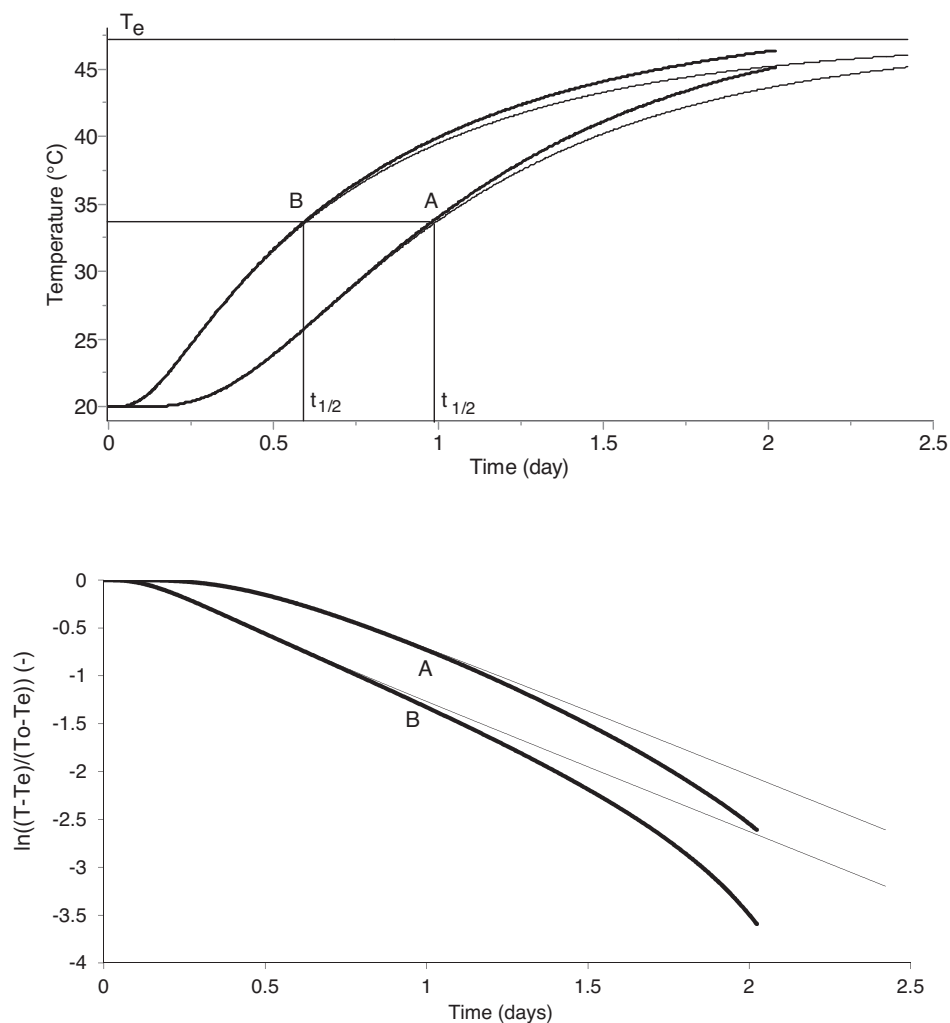| U (W m^{-2} K^{-1})	Sample mass									
	50 kg					0.285 kg				
	Heat loss (mW kg^{-1} K^{-1})					Heat loss (mW kg^{-1} K^{-1})				
	SADT (°C)	FUTD and time lag	FUTD and no time lag	FUTD and no time lag and inert	HCT	SADT (°C)	FUTD and time lag	FUTD and no time lag	FUTD and no time lag and inert	HCT
10	47.54	26	34	27	14	59.28	542	616	551	310
		35	37	27	25		607	631	551	456
5	47.17	23	30	24	13	58.75	382	427	376	238
		30	33	24	21		411	429	376	316
2	46.52	19	23	18	10	57.29	205	218	189	143
		22	24	18	15		210	216	189	169
1	45.79	14	17	13	8	54.73	114	118	103	87
		16	17	13	11		115	117	103	96
0.5	45.08	9	10	8	6	51.65	60	61	54	49
		10	10	8	7		60	61	54	52
0.4	44.85	8	9	7	5	50.6	48	50	43	40
		8	9	7	6		49	49	43	42
0.3	44.58	6	7	5	4	49.54	37	38	33	31
		6	7	5	5		37	37	33	33
0.2	44.35	5	5	4	3	47.86	25	25	22	21
		5	5	4	3		25	25	22	22
0.1	44.28	3	3	2	2	46.04	13	13	11	11
		3	3	2	2		13	13	11	11
0.05	44.36	1	2	1	1	45.07	7	7	6	6
		1	2	1	1		7	7	6	6

Fig. 9. (Top) Simulated temperature-time dependences during the heating of 50 kg of AIBN in a cylindrical container with $H/D = 1$. The curves are calculated for the sample center (A) ($R = 0$; $H/2$) and the position (B) ($R/2$; $H/4$). The bold and thin curves represent the temperature-time dependence for the cases when the heat generated by the reaction is considered (bold) or neglected. (Bottom) Semi-log plot of the fractional unaccomplished temperature difference vs. time (FUTD-method) simulated for both positions of the temperature sensors.
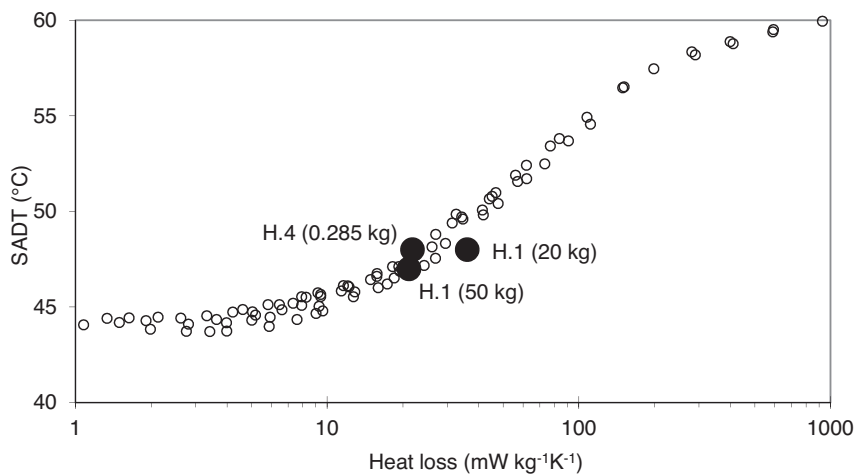

Fig. 10. Dependence of SADT computed with the kinetic based approach for all pairs of m ($0.1 \leq m \leq 250$ kg) and U ($0.05 \leq U \leq 10$ W m^{-2} K^{-1}) presented in Table 4 (small symbols) and measured according to the UN tests using sample masses of 0.285 (H.4), 20.25 (H.1) and 50 (H.1) kg (large filled symbols) on the heat loss values. Observed scattering at lower heat loss values compensates the deviations resulted from different methods of heat loss calculation presented in Table 5.

The reported results in Table 5 illustrate the influence of the sample mass m and overall heat transfer coefficient U on the SADT values. For an overall heat transfer coefficient of $U = 5\,\mathrm{W\,m^{-2}\,K^{-1}}$, the increase of the mass from 0.285 to 50 kg results in the decrease of the SADT values from 58.75 °C to 47.17 °C, respectively. The differences of the heat loss values in the sample center ($R = 0$; $H/2$) and in the position ($R/2$; $H/4$) are the largest when calculated with the HCT-method. Heat loss values calculated by this method are lower compared to those derived from the FUTD-method. In general, observed differences decrease for smaller heat loss values. As expected, the cooling coefficients are independent of the position in the material, when determined with the FUTD-method without considering the time lag and any heat release i.e., like in an inert material or at $T_e \ll$ SADT. Therefore, only values calculated by this method are further considered.

The influence of the change of overall heat transfer coefficient U is smaller for larger packaging sizes, with 50 kg the decrease of U from 5 to 0.05 $\mathrm{W\,m^{-2}\,K^{-1}}$ results in the decrease of the SADT values from 47.17 °C to 44.36 °C, whereas for 0.285 kg, the same 100-fold decrease of overall heat transfer coefficient results in the decrease of the SADT values from 58.75 °C to 45.07 °C. The simulation results presented in Table 5 indicate that a package of 50 kg of AIBN with an overall heat transfer coefficient of 5 $\mathrm{W\,m^{-2}\,K^{-1}}$ with heat loss of 24 $\mathrm{W\,kg^{-1}\,K^{-1}}$ and 0.285 kg of AIBN placed in Dewar with similar heat loss value of 22 $\mathrm{W\,kg^{-1}\,K^{-1}}$ with $U = 0.2\,\mathrm{W\,m^{-2}\,K^{-1}}$ have a similar SADT in the range of 47–48 °C.

Fig. 10 depicts the relationship (for all pairs of m: $0.1 \leq m \leq 250\,\mathrm{kg}$ and U: $0.05 \leq U \leq 10\,\mathrm{W\,m^{-2}\,K^{-1}}$ presented in Table 4), between computed SADT values (small open circles) determined for cylinders with $H/D = 1$ with the kinetic based method and their corresponding heat loss values calculated by the FUTD-method (as presented in Table 5). The similarity of the heat loss values of the packages filled with various amount of AIBN results in similar SADT values. The large filled circles in Fig. 10 present the experimental results of SADT determination for samples masses of 20.25 and 50 kg evaluated from the real-scale H.1-test and for sample mass of 285 g from the H.4 test with Dewar. The similarity between the experimental results obtained by BAM (large filled symbols) and

the simulation data (smaller circles) fully validates the method of SADT evaluation based on the kinetic approach.

The SADT values determined by BAM according to UN test H.1 procedure amount to 48 and 47 °C for 20 and 50 kg packages of AIBN, respectively. These values are consistent with the results of UN SADT test H.4 performed in Dewar with 285 g of AIBN. Fig. 11 presents the experimental T–t dependences and runaway events obtained for surrounding temperatures of 45 and 48 °C. As confirmed by our simulations (see Table 5 and Fig. 10) the heat loss similarity ensured the similar thermal behavior as in the large-scale H.1 test due to the proper selection of both, sample mass and Dewar type.

6. Determination of SADT based on merging DSC data with large-scale test (Case 'S & S')

The following chapter presents the basic principles of a new kinetic analysis workflow in which the heat flow traces (e.g., DSC) are merged with results of large-scale tests as e.g., H.1 or H.4. As it has been presented in the previous chapters, a differential isoconversional analysis (Eq. (7)) can be applied to obtain a precise kinetic description of the reaction measured by DSC. Evaluated dependences of the activation energy $E(\alpha)$ and $A(\alpha)f(\alpha)$ on the reaction progress α denote an approximate trend behavior as clearly seen in Fig. 3A. It can be assumed that in small conversion ranges $\Delta\alpha$ the apparent activation energy $E(\alpha)$ and the term $A(\alpha)f(\alpha)$ do not change significantly so that their ratio can be considered as approximately constant and we can write:

$$\ln(A(\alpha)f(\alpha)) \cong CE(\alpha) \qquad (26)$$

where C denotes a constant of proportionality. Similar approach is widely used when applying the integral isoconversional method for the determination of the activation energy $E(\alpha)$ by integration over a small segment of $\Delta\alpha$ [46]. It is generally recommended to compute the $E(\alpha)$ values with a step of $\Delta\alpha$ not larger than 0.05 and to report the resulting dependencies of $E(\alpha)$ vs. α. Because the criterion of SADT of AIBN with an overheat of 6 °C ($\Delta T6$) is fulfilled already at the beginning of the decomposition when the reaction progress α amounts to ca. 3% only (see Figs. 4 and 5, left column),
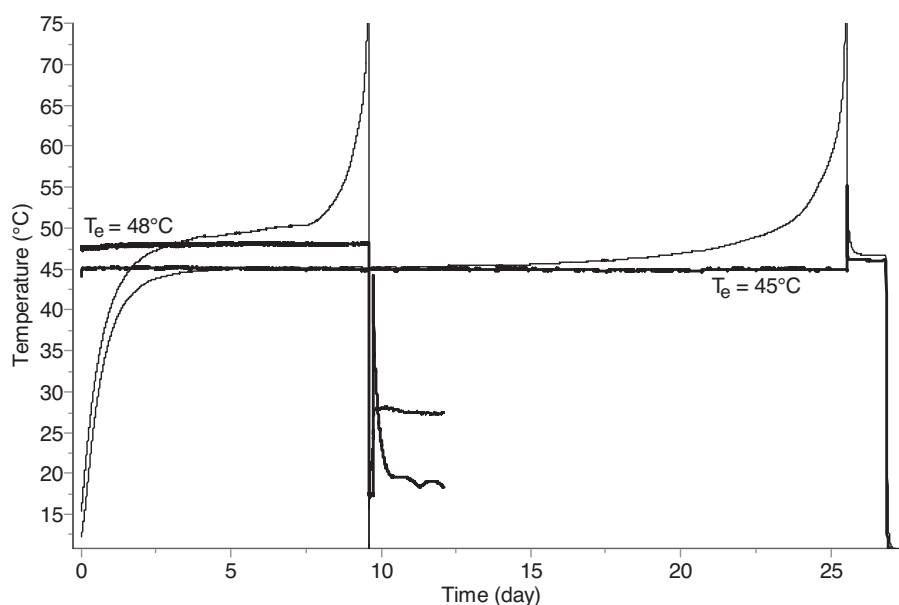

Fig. 11. UN SADT test H.4 of 285 g of AIBN performed by BAM in a Dewar. SADT amounts to 48 °C. The rapid temperature rise (thermal runaway) was observed after ca. 9.5 and 25.5 days for the surrounding temperatures of 48 °C and 45 °C, respectively. The respective surrounding and center temperatures are depicted by the bold and thin lines, respectively.
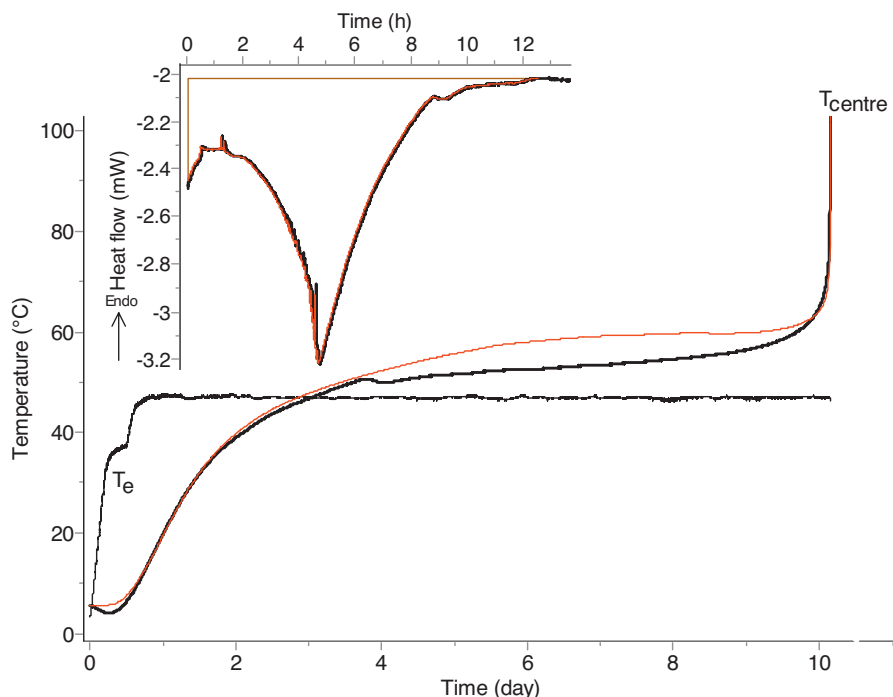
Fig. 12. Experimental (black) vs. simulated (red): temperature in the center of 50 kg AIBN in a drum (filling height $H = 46$ cm and $D = 46$ cm) with corresponding thermal runaway event. The calculations were done using the newly introduced kinetic approach based on merging DSC signal with temperature-time dependence recorded in large-scale test under the assumption of Eq. (26). The real temperature course of the ambient temperature T_e is applied in the simulation. Experimental (black) and simulated (red) DSC traces at 80 °C of 14.5 mg of AIBN are presented in the inset.

Eq. (26) may be also applicable for the SADT evaluation due to considering of relatively very narrow conversion range. Integration in small α segments yields $E(\alpha)$ values that are practically identical with those obtained by the differential isoconversional analysis (Eq. (7)) which rewritten in logarithmic form gives

$$\ln\left(\frac{d\alpha}{dt_\alpha}\right) = \ln(A(\alpha)f(\alpha)) - \frac{E(\alpha)}{R}\frac{1}{T(t_\alpha)} \qquad (27)$$

and by considering Eq. (26) leads to the following expression

$$\ln\left(\frac{d\alpha}{dt_\alpha}\right) \cong E(\alpha)\left(C - \frac{1}{RT(t_\alpha)}\right) \qquad (28)$$

After final recombination of Eq. (28), one obtains the following expression allowing evaluation of the activation energy $E(\alpha)$

$$E(\alpha) \cong \frac{\ln(d\alpha/dt_\alpha)}{C - \frac{1}{RT(t_\alpha)}} \qquad (29)$$

The numerical estimation of the parameter C can be done by comparing the reaction progress α of the DSC signal (e.g., measured at 80 °C for AIBN, Fig. 12 inset) and the time of the runaway event in a large-scale test (e.g., H1-test with 50 kg in a drum, Fig. 12) with their simulated courses using the adequate expression for the heat balance (Eqs. (10), (12)–(14)). In the simulation we applied the real temperature course of the ambient temperature (depicted as T_e in Figs. 6 and 12) according to BAM data. The assumption that the furnace temperature is supposed to be constant from the beginning of the experiment can significantly influence the correctness of the simulations. During the approximation of the C value, its increase or decrease results in shifting the runaway event (large-scale test) towards longer or shorter times, respectively. The best fit was obtained for the value of

$C = 2.81\text{E} - 4\text{ mol J}^{-1}$. Excluding the heat of reaction which was taken for the heat flow curve recorded at 80 °C ($\Delta H_r = -1128.2\text{ J g}^{-1}$, see Fig. 2), all other parameters used for the packaging and physical properties of AIBN are the same as those used during the simulations presented in Fig. 4. Once the optimal value for C is determined, the activation energy $E(\alpha)$ and the term $A(\alpha)f(\alpha)$ can be calculated as a function of the reaction progress α using Eqs. (26) and (29). The time to runaway of the large-scale test can be then obtained by numerical integration using either Eqs. (10) or (12)–(14) depending on the physical state of the material. The large scale-test which may be used for a simultaneous consideration (merging) with DSC data can be either an H.1 or H.4 test and at a temperature exceeding the supposed SADT value in order to monitor a runaway event. Fig. 12 depicts the simulations based on described approach and experimental traces of the heat flow recorded by DSC for the AIBN sample at 80 °C (inset) and the runaway event for 50 kg of AIBN in a drum, respectively. It is seen that both, the experimental heat flow signal and the large-scale test are well fitted by simulated traces. For the the sample masses of 50 kg (drum, $H = D = 46$ cm), 20.25 kg (box, 39 cm × 29 cm × 26 cm) and 5.05 kg (box, 29 cm × 22 cm × 16 cm), SADT values computed with this new "merging" approach amount to 46.02, 49.03 and 53.89 °C, respectively. These values are very close to those obtained experimentally in large-scale UN tests H.1 which are given in text and in Table 3. The proposed new procedure, based on computing kinetic parameters from at least one large- and one small-scale test enables a considerable decrease of the amount of large-scale tests necessary for SADT determination. Since in our proposal the results evaluated from DSC data are combined with those from any large-scale test, this new approach for SADT determination is potentially more accurate than those based on small-scale experiments and much less expensive and time consuming than those based on large-scale tests only. For merging mg- with kg-scale experiments, one can also use the experimental

data collected with calorimeters such as C80 or TAM which are more sensitive than conventional DSC devices.

7. Conclusion

The comparison of the methods for determining the thermal hazard properties of reactive chemicals from DSC traces and from United Nations SADT test H.1 and H.4 is illustrated by the results of SADT simulations performed with Azobisisobutyronitrile (AIBN). For the materials in which melting occurs before or during the decomposition, it may be incorrect to use the kinetic parameters and heat balance computed for the liquid state for the prediction of the reaction kinetics and thermal behavior in the solid phase [4,6]. In such a situation, the experiments should be performed isothermally at temperatures below the melting point. In the present study, the kinetics of decomposition of AIBN in the solid state was investigated in a narrow temperature window of 80-90 °C, just below the sample melting. The results of DSC experiments were elaborated by AKTS-Thermokinetics software [30]. The kinetic parameters of the decomposition were evaluated by a "model-free" (differential isoconversional) kinetic analysis method, because the mechanism of AIBN decomposition is not fully known and "model-based" kinetic analysis for comparison. Application of the kinetic parameters, together with the heat balance performed by numerical analysis, allowed scale-up of the thermal behaviour from mg- to kg-scale and simulation of SADT. Additionally, this study presents the evaluation of the influence of the overall heat transfer coefficient U on the SADT value. The obtained results for limited cylinders with given H/D ratio (H: height, D: diameter) and flat lids (e.g. drums) clearly illustrate the dependence of SADT on the sample mass. Influence of the other container shapes (cube and sphere) on SADT values was additionally presented. The simulated results indicate that the SADT values of AIBN do not significantly depend on the considered container shapes. Because in practice the SADT values are rounded to the next higher multiple of 5 °C [1], the observed differences support the use of spherical shapes in the first approximation of SADT determination.

The AKTS-Thermal Safety software [30] and the kinetics-based approach can be used for proper selection of experimental conditions for SADT testing. SADT values for AIBN obtained in this study and those presented for other materials [45] indicate that software-based calculations with the correct kinetic approach and appropriate heat balance allow the successful scale-up of thermal behaviour from mg- to kg-scale. Determined SADT values were verified experimentally with a series of large-scale experiments (UN test H.1 [1]) performed with packaging of 5, 20 and 50 kg of AIBN in an oven at constant temperatures. Additionally, the results of small-scale test H.4 for SADT determination based on the heat loss similarity as described in details in the UN Manual [1] were compared with the simulated data based on kinetic approach. Results of our simulations taking into account the issue of the heat loss similarity indicate that it is recommended to use the FUTD-method instead of the HTC-method. Such a procedure provides a more accurate value of the cooling coefficient required for the calculation of the heat loss necessary for scale-up. The main advantage of the FUTD-method consists in its ability to measure the heat loss values independently of the position of the thermocouple in the material. SADT values for AIBN obtained in this study either using the large-scale test H.1 (kg-scale), the small-scale test H.4 (g-scale) or the kinetic based approach (mg-scale) and those presented for other materials [27,28,37,45] indicate the usefulness of the test method based on DSC experiments, in which significantly smaller amounts of reactive materials are used. The results of the application of a newly proposed kinetic approach in which DSC traces are considered simultaneously with results of large-scale tests (e.g. H.1 or H.4) indicate its usefulness. The simulated SADT values obtained by applying this merging approach are very close to the SADT values obtained experimentally in large-scale experiments. Use of a newly proposed kinetic workflow may increase accuracy of simulations of SADT based on results collected in mg-scale and decrease the amount of expensive and time consuming experiments in kg-scale tests.

References

[1] United Nations, UN Recommendations on the Transport of Dangerous Goods Manual of Tests and Criteria, 5th ed., United Nations, New York and Geneva, 2009, pp. 297–316.
[2] M.E. Brown, M. Maciejewski, S. Vyazovkin, R. Nomen, J. Sempere, A. Burnham, J. Opfermann, R. Strey, H.L. Anderson, A. Kemmler, R. Keuleers, J. Janssens, H.O. Dessseyn, Chao-Rui Li, B. Tong Tang, B. Roduit, J. Malek, T. Mitsuhashi, Computational aspects of kinetic analysis. Part A: the ICTAC kinetics project-data, methods and results, Thermochim. Acta 355 (2000) 125–143.
[3] S. Vyazovkin, A.K. Burnham, J.M. Criado, L.A. Pérez-Maqueda, C. Popescu, N. Sbirrazzuoli, ICTAC Kinetics Committee recommendations for performing kinetic computations on thermal analysis data, Thermochim. Acta 520 (2011) 1–19.
[4] S. Vyazovkin, K. Chrissafis, M.L. Di Lorenzo, N. Koga, M. Pijolat, B. Roduit, N. Sbirrazzuoli, J.J. Suñol, ICTAC Kinetic Committee recommendations for collecting experimental thermal analysis data for kinetic computations, Thermochim. Acta 590 (2014) 1–23.
[5] M. Malow, K.-D. Wehrstedt, M. Manolov, Thermal decomposition of AIBN. Part A: decomposition in real scale packages and SADT determination, Thermochim. Acta (2015) (submitted to publication).
[6] B. Roduit, M. Hartmann, P. Folly, A. Sarbach, P. Brodard, R. Baltensperger, Determination of thermal hazard from DSC measurements. Investigation of self accelerating decomposition temperature (SADT) of AIBN, J. Therm. Anal. Calorim. 117 (2014) 1017–1026.
[7] J. Farjas, P. Roura, Simple approximate analytical solution for nonisothermal single-step transformations: kinetic analysis, AIChE J. 54 (2008) 2145–2154.
[8] P. Šimon, Fourty years of the Šesták–Berggren equation, Thermochim. Acta 520 (2011) 156–157.
[9] L.A. Pérez-Maqueda, J.M. Criado, P.E. Sànchez-Jiménez, Combined kinetic analysis of solid-state reactions: a powerful tool for the simultaneous determination of kinetic parameters and the kinetic model without previous assumptions on the reaction mechanism, J. Phys. Chem. A10 (2006) 12456–12462.
[10] J. Šesták, G. Berggren, Study of the kinetics of the mechanism of solid-state reactions at increasing temperatures, Thermochim. Acta 3 (1971) 1–12.
[11] B. Roduit, M. Hartmann, P. Folly, A. Sarbach, R. Baltensperger, Prediction of thermal stability of materials by modified kinetic and model selection approaches based on limited amount of experimental points, Thermochim. Acta 579 (2014) 31–39.
[12] M.R. Kamal, Thermoset characterization for moldability analysis, Polym. Eng. Sci. 14 (1974) 231–239.
[13] S. Sourour, M.R. Kamal, Differential scanning calorimetry of epoxy cure: isothermal cure kinetics, Thermochim. Acta 14 (1976) 41–59.
[14] M.A. Watzky, A.M. Morris, E.D. Ross, R.G. Finke, Fitting yeast and mammalian prion aggregation kinetic data with the Finke–Watzky two-step model of nucleation and autocatalytic growth, Biochemistry 47 (2008) 10790–10800.
[15] A.M. Morris, M.A. Watzky, R.G. Finke, Protein aggregation kinetics, mechanism, and curve-fitting: a review of the literature, Biochim. Biophys. Acta 1794 (2009) 375–397.
[16] E.G. Prout, F.C. Tompkins, The thermal decomposition of potassium permanganate, Trans. Faraday Soc. 40 (1944) 488–498.
[17] E.G. Prout, F.C. Tompkins, The thermal decomposition of silver permanganate, Trans. Faraday Soc. 42 (1946) 468–472.
[18] M.E. Brown, The Prout–Tompkins rate equation in solid-state kinetics, Thermochim. Acta 300 (1997) 93–106.
[19] M.E. Brown, B.D. Glass, Pharmaceutical applications of the Prout–Tompkins rate equation, Int. J. Pharm. 190 (1999) 129–137.
[20] M.A. Bohn, Prediction of life times of propellants—improved kinetic description of the stabilizer consumption, Propellants Explos. Pyrotech. 19 (1994) 266–269.
[21] M.A. Bohn, Prediction of in-service time period of three differently stabilized single base propellants, Propellants Explos. Pyrotech. 34 (2009) 252–266.
[22] M.A. Bohn, The Prout–Tompkins problem and its solution, Proceedings of 42nd International Annual Conference, ICT, Karlsruhe, Germany, 2011, pp. 1–19 (paper 52).
[23] N. Eisenreich, A. Pfeil, Non-linear least-squares fit of non-isothermal thermoanalytical curves. Reinvestigation of the kinetics of the autocatalytic decomposition of nitrated cellulose, Thermochim. Acta 61 (1983) 13–21.
[24] J. Krstina, G. Moad, I. Willing, S.K. Danek, D.P. Kelly, S.L. Jones, D.H. Solomon, Further studies on the thermal decomposition of AIBN-implications concerning the mechanism of termination in methacrylonitrile polymerization, Eur. Polym. J. 29 (1993) 379–388.

[25] G. Xu, R.P. Nambiar, F.D. Blum, Room-temperature decomposition of 2,2'-azobis(isobutyronitrile) in emulsion gels with and without silica, J. Colloid Interf. Sci. 302 (2006) 658–661.

[26] H.L. Friedman, Kinetics of thermal degradation of char-forming plastics from thermogravimetry. Application to a phenolic plastic, J. Polym. Sci. Pol. Lett. 6 (1964) 183–195.

[27] B. Roduit, P. Folly, B. Berger, J. Mathieu, A. Sarbach, H. Andres, M. Ramin, B. Vogelsanger, Evaluating SADT by advanced kinetics-based simulation approach, J. Therm. Anal. Calorim. 93 (2008) 153–161.

[28] B. Roduit, L. Xia, P. Folly, B. Berger, J. Mathieu, A. Sarbach, H. Andres, M. Ramin, B. Vogelsanger, D. Spitzer, H. Moulard, D. Dilhan, The simulation of the thermal behaviour of energetic materials based on DSC and HFC signals, J. Therm. Anal. Calorim. 93 (2008) 143–152.

[29] B. Roduit, M. Odlyha, Prediction of thermal stability of fresh and aged parchment, J. Therm. Anal. Calorim. 85 (2006) 157–164.

[30] AKTS-Thermokinetics and AKTS-Thermal Safety Software, http://www.akts.com.

[31] N.N. Semenov, Thermal theory of combustion and explosion, Progress in Physics and Science U.S.S.R, 23 (1940) 251–292, 1024, National Advisory Committee for Aeronautics, Washington, 1942, pp. 1–57 (Technical memorandum).

[32] D.A. Frank-Kamenetskii, Diffusion and Heat Transfer Chemical Kinetics, 2nd ed., Plenum Press, New York-London, 1969, pp. 375 (translated from Russian by J.P. Appleton).

[33] S. Guo, W. Wan, C. Chen, W.H. Chen, Thermal decomposition kinetic evaluation and its thermal hazards prediction of AIBN, J. Therm. Anal. Calorim. 113 (2013) 1169–1176.

[34] M. Malow, H. Michael-Schulz, K.D. Wehrstedt, Evaluative comparison of two methods for SADT determination (UN H.1 and H.4), J. Loss Prevent. Proc. 23 (2010) 740–744.

[35] M.W. Whitmore, J.K. Wilberforce, Use of the accelerating rate calorimeter and the thermal activity monitor to estimate stability temperatures, J. Loss Prevent. Proc. 6 (1993) 95–101.

[36] T. Kotoyori, Critical temperatures for the thermal explosion of chemicals, Industrial Safety Series, vol. 7, Elsevier, 2005, pp. 48362.

[37] B. Roduit, C. Borgeat, B. Berger, P. Folly, B. Alonso, J.N. Aebischer, The prediction of thermal stability of self-reactive chemicals. From milligrams to tons, J. Therm. Anal. Calorim. 80 (2005) 91–102.

[38] J.M. Bessière, B. Boutevin, O. Loubet, Determination of kinetic parameters for isothermal decomposition of azo initiators of polymerization by differential scanning calorimetry, Polym. Bull. 30 (1993) 545–549.

[39] J.M. Bessière, B. Boutevin, O. Loubet, Détermination des paramètres cinétiques et thermodynamiques des amorceurs de polymérisation radicalaire de type azoïque par enthalpimétrie différentielle en mode isotherme, Eur. Polym. J. 30 (1994) 813–820.

[40] N.D. Lebedeva, N.M. Gutner, Y.A. Katin, N.M. Kozlova, N.N. Kiseleva, E.F. Makhina, S.L. Dobychin, Thermochemical study of bis-hydroxyethylpiperazine, N,N-dimethylpropylendiamine and 2,2-azodiisobutyrodinitrile, J. Appl. Chem. USSR 57 (1984) 2118–2122.

[41] W.S. McEwan, M.W. Rigg, The heats of combustion of compounds containing the tetrazole ring, J. Am. Chem. Soc. 73 (1951) 4725–4727.

[42] M. Steensma, P. Schuurman, M. Malow, U. Krause, K.D. Wehrstedt, Evaluation of the validity of the UN SADT H.4 test for solid organic peroxides and self-reactive substances, J. Hazard. Mater. A117 (2005) 89–102.

[43] M. Steensma, P. Schuurman, W.A. Mak, Validation of the UN criteria for the uncooled sea transport of liquid organic peroxides: full-scale test and modeling, J. Loss Prevent. Proc. 21 (2008) 635–641.

[44] H. Fierz, Influence of heat transport mechanisms on transport classification by SADT-measurement as measured by the Dewar-method, J. Hazard. Mater. A96 (2003) 121–126.

[45] M. Dellavedova, C. Pasturenzi, L. Gigante, A. Lunghi, Kinetic evaluations for the transportation of dangerous chemical compounds, Chem. Ing. Trans. 26 (2012) (2011) 585–590.

[46] S. Vyazovkin, Modification of the integral isoconversional method to account for variation in the activation energy, J. Comput. Chem. 22 (2001) 178–183.